

University of Louisville

ThinkIR: The University of Louisville's Institutional Repository

Electronic Theses and Dissertations

8-2011

Profile of systemic treatment with the antiviral lectin Griffithsin in guinea pigs.

Christopher Lynn Barton 1976-
University of Louisville

Follow this and additional works at: <https://ir.library.louisville.edu/etd>

Recommended Citation

Barton, Christopher Lynn 1976-, "Profile of systemic treatment with the antiviral lectin Griffithsin in guinea pigs." (2011). *Electronic Theses and Dissertations*. Paper 79.
<https://doi.org/10.18297/etd/79>

This Master's Thesis is brought to you for free and open access by ThinkIR: The University of Louisville's Institutional Repository. It has been accepted for inclusion in Electronic Theses and Dissertations by an authorized administrator of ThinkIR: The University of Louisville's Institutional Repository. This title appears here courtesy of the author, who has retained all other copyrights. For more information, please contact thinkir@louisville.edu.

PROFILE OF SYSTEMIC TREATMENT WITH THE ANTIVIRAL LECTIN
GRIFFITHSIN IN GUINEA PIGS

By

Christopher Lynn Barton
B.A., University of Louisville, 1998
J.D., University of Louisville, 2002

A Thesis
Submitted to the Faculty of the
School of Medicine of the University of Louisville
In Partial Fulfillment of the Requirements
For the Degree of

Master of Science

Department of Pharmacology and Toxicology
University of Louisville

Louisville, KY

August 2011

Copyright 2011 by Christopher Lynn Barton

All rights reserved

PROFILE OF SYSTEMIC TREATMENT WITH THE ANTIVIRAL LECTIN
GRIFFITHSIN IN GUINEA PIGS

By

Christopher Lynn Barton
B.A., University of Louisville, 1998
J.D., University of Louisville, 2002

A Thesis Approved on

May 25, 2011

By the following Thesis Committee:

Kenneth E. Palmer, Ph.D.

Theresa Chen, Ph.D.

Harrell Hurst, Ph.D.

J. Brad Chaires, Ph.D.

DEDICATION

This thesis is dedicated to my partner

Christopher L. Dennison

who supports me in all of my endeavors, without hesitation.

ABSTRACT

PROFILE OF SYSTEMIC TREATMENT WITH THE ANTIVIRAL LECTIN GRIFFITHSIN IN GUINEA PIGS

Christopher Lynn Barton

May 25, 2011

Griffithsin (GRFT) is a carbohydrate binding protein derived from the red alga *Griffithsia sp.* that has been shown to effectively interfere with the cellular attachment and infectivity of a number of viruses, including HIV-1. However, it is currently unknown what impact systemic GRFT administration may have upon a biological system. For initial *in vivo* testing, we introduced GRFT into guinea pigs (*Cavia Porcellus*) via subcutaneous injection. Based on histological, serological, and biochemical data derived from these experiments, GRFT is well tolerated and maintained at physiologically relevant concentrations while retaining its potent antiviral activity. Follow up *in vitro* testing included a number of assays to assess GRFT's interaction with serum proteins and proteases. The results confirm that GRFT is well tolerated by animals and maintains its antiviral activity while simultaneously displaying a strong resistance to proteolytic cleavage. Accordingly, GRFT is a strong candidate for further development as a systemic anti-viral therapy.

TABLE OF CONTENTS

PAGE

DEDICATION.....	iii
ACKNOWLEDGEMENTS.....	iv
ABSTRACT.....	v
LIST OF FIGURES.....	viii
CHAPTER 1: INTRODUCTION.....	1
CHAPTER 2: ASSESS GRFT'S SHORT TERM SYSTEMIC TOLERABILITY, ANTI-VIRAL ACTIVITY, AND SERUM PERSISTENCE IN THE ABSENCE OF AN ANTIBODY RESPONSE.....	19
INTRODUCTION.....	19
MATERIALS AND METHODS.....	21
RESULTS.....	27
CONCLUSIONS AND FUTURE DIRECTIONS.....	41
CHAPTER 3: CHARACTERIZATION OF BIOCHEMICAL INTERACTIONS OF GRFT BY EXAMINING ITS IMPACT UPON SERUM PROTEIN PROFILES AND GRFT-PROTEASE INTERACTIONS.....	43
INTRODUCTION.....	43
MATERIALS AND METHODS.....	47
RESULTS.....	54
CONCLUSIONS AND FUTURE DIRECTIONS.....	64

CHAPTER 4: ANALYSIS OF GRFT RESISTANT HIV STRAIN AND GENERATION OF HIV-ENV PSEUDOVIRUS TO DETERMINE GRFT NEUTRALIZATION CAPCACITY...	67
INTRODUCTION.....	67
MATERIALS AND METHODS	70
RESULTS	73
CONCLUSIONS AND FUTURE DIRECTIONS.....	78
CHAPTER 5: OVERALL RESEARCH IMPLICATIONS AND APPLICATIONS.....	80
REFERENCES	83
APPENDIX	90
CURRICULUM VITA.....	93

LIST OF FIGURES

FIGURE	PAGE
1.1 N-linked glycans – structural arrangements of subtypes.....	17
1.2 Steps of HIV-1 cellular entry highlighting sites of potential therapeutic Interventions.....	18
2.1 Concentrations of GRFT in serum and vaginal washes of guinea pigs treated with GRFT or PBS.....	32
2.2 Analysis of HIV neutralization activity of guinea pig serum and vaginal wash samples.....	34
2.3 Mean whole body weight gain increases during treatment with PBS, GRFT, or GRFT ^{lec-}	37
2.4 Mean organ weight- to-total bodyweight percentages of treatment groups.....	38
3.1 Mean serum thermograms of guinea pigs groups treated with GRFT, GRFT ^{lec-} , or PBS.....	57
3.2 Thermograms of human serum spiked with varying concentrations of GRFT.....	58
3.3 Thermograms of human serum spiked with varying concentrations of GRFT ^{lec-}	59

3.4	Selected mass spectra of GRFT digestions.....	61
4.1	Potential N-linked glycosylation sites of gp120 of Du156.12 and Du156.R18.....	76
4.2	Pseudovirus titer of Du156.12 in TZM-bl cells.....	77

CHAPTER 1

INTRODUCTION

As the spread of viruses such as HIV, HCV, SARS and influenza continues throughout the world, it is imperative that new therapies are fully explored as potential weapons for stemming further transmission to uninfected individuals as well as treating those already infected. HIV, affecting approximately 33 million people worldwide, claims the lives of roughly 2 million people per year [1]. HCV, the most common blood born infection in the US, currently affects 3-4 million people, and is the leading cause of liver transplantation [2]. A common structural feature among all of these viruses is a dense, high-mannose N-linked glycan shield used to evade host immune responses and stabilize viral envelope structure [3-5]. Accordingly, agents that can target clusters of high-mannose glycans, typical of many viral envelopes, are highly attractive candidates for potential antiviral therapies.

Among some of the most promising and potent topical anti-microbial agents currently being investigated to prevent transmission of HIV, HCV, SARS, and influenza are a subset of natural product derived lectins, carbohydrate binding proteins which bind to the envelope glycoproteins of many viruses, including HIV [6-9]. It is believed that these antiviral lectins can inhibit viral transmission by selectively binding to the N-linked mannose moieties present on

the surface of the viral envelope, thus preventing viral entry [7, 10-12]. Griffithsin (GRFT), derived from the red algae *Griffithsia sp.*, is one such lectin that is currently under investigation as a potential vaginal microbicide [13]. *In vitro* studies indicate that GRFT is a particularly potent HIV-1 entry inhibitor, with an average EC₅₀ of 40 pM [14].

In addition to direct binding activity on free virions, it has been demonstrated *in vitro* that antiviral lectins, such as GRFT, can interfere with and prevent cell-to-cell transmission of HIV between dendritic cells and macrophages [13]. This ability to interfere with cell-to-cell viral transmission, as well as its ability to effectively bind to the GP120 of HIV viral particles, warrants an investigation into whether GRFT, in addition to its potential usage as a topical antimicrobial, has utility as a systemic treatment for HIV.

The goal of this Master's thesis is to explore the potential of using GRFT as a systemic therapy for enveloped viruses possessing high mannose N-linked glycans by examining its systemic tolerability in guinea pigs, as well as investigating some of the biological interactions that GRFT may encounter during the course of systemic treatment. In Chapter 2, we assess GRFT's impact upon metabolic organ systems and examine GRFT's serum persistence and anti-viral activity when injected subcutaneously into guinea pigs. Chapter 3 explores biochemical interactions that GRFT may have when introduced into systemic circulation, including exposure to proteases and potential endogenous binding targets. Finally, in Chapter 4, we analyze a viral resistance profile in the context of HIV-1, examining glycosylation site changes that occur in a GRFT-resistant

HIV isolate. Also described is the process by which HIV-1 enveloped pseudovirus particles can be generated for examining GRFT's neutralization capacity.

Glycosylation States

Glycosylation is the process by which complex carbohydrate chains are enzymatically added to organic molecules, such as proteins and fats [15]. These carbohydrate chain additions serve as essential factors in maintaining proper protein folding, increase protein stability, and contribute to their functionality [16]. Furthermore, glycosylation can greatly affect the water solubility of proteins, given that the addition of the carbohydrate chains results in greater hydrophilicity. In the case of viruses, glycosylation changes of external proteins and lipids can greatly impact infectivity and viral fitness [17].

Occurring in either the golgi apparatus or the endoplasmic reticulum, glycosylation can result in five different types of glycans: N-linked, O-linked, C-linked, glipiated, or phospho-glycans. The type of glycosylation most relevant to the studies of GRFT are of the N-linked variety. Beginning with the addition of a 14 unit oligosaccharide precursor to an asparagine in a polypeptide chain, N-linked glycosylation is signaled by either the sequence Asn-X-Ser or Asn-X-Thr, where X can be any amino acid except proline [18]. As a structural precursor common to most eukaryotes, the general branched carbohydrate chain contains 3 glucose, 9 mannose, and 2 *N*-acetylglucosamine molecules. Subsequently, this branched carbohydrate chain is attached to a carrier molecule called a dolichol, and transferred to the appropriate signal sequence (NXS/T) on the polypeptide chain as it is translocated into the ER lumen [19].

In addition to the varying linkage types available for glycosylation, there are also differences in sugar compositions between glycans of the same linkage type. These differences can result in the following sub-types of glycans: High-mannose, Hybrid, or Complex (Fig.1.1). These different subsets vary in the amount of n-acetylglucosamine presented on the terminal portions of the sugar. Whether an oligosaccharide will ultimately be High-mannose, Complex or Hybrid is thought to depend on its accessibility to saccharide-modifying proteins in the Golgi. High-Mannose glycans are a type of the N-glycan chain added to certain asparagine residues of secreted or membrane proteins in eukaryotic cells, containing 5-9 mannose residues [15]. High-mannose glycans are the initial state of glycosylation for many glycans, with further editing occurring in the Golgi which results in the formation of hybrid and complex glycans.

The final, terminal structure of the glycan after editing determines its subtype. In the case of High-mannose glycans, no n-acetylglucosamines are presented, resulting in exclusively mannose terminals (Fig. 1.1A). In the case of Hybrid glycans, enzymatic activity results in a carbohydrate chain that possesses at least one terminal N-acetylglucosamine and at least one terminal mannose (Figure 1.1B). However, in the case Complex N-linked glycans, enzymatic activity results in a carbohydrate chain containing multiple terminal N-acetylglucosamines (Fig.1.1C). Deficiencies in certain key modification enzymes can greatly affect glycosylation profiles. For example, reduction in activity of cellular N-acetylglucosaminyltransferase I (GnT-I) – a glycan editing

enzyme - can result in the production of almost entirely High-mannose type glycans [20].

HIV-1

HIV-1, the virus responsible for AIDS, is a lentivirus belonging to the retrovirus family of viruses [21]. Genetically, the HIV genome contains a total of nine genes which can code for a number of viral proteins [22]. Three of them encode structural and functional proteins essential for new virions: Gag, Pol, and Env [22]. These three genes code precursor proteins which must be further processed by cleavage before they become functional. Six other genes- tat, rev, nef, vif, vpr and vpu-code for various virion processing mechanisms, including cellular transport, assembly, and budding [22].

Gag encodes a precursor protein which is cleaved into four proteins: matrix (p17), capsid (p24), neocapsid (p7), and p6 proteins [22]. This group is synthesized as the p55 polyprotein which is subsequently cleaved by viral protease into their individual components as well as two spacer proteins, p1 and p2 [22]. These individual proteins are involved in virion core structure, assembly, and budding.

Pol genes also code for the synthesis of a single unit precursor protein which is cleaved to produce viral protease, reverse transcriptase and integrase [22]. These proteins are packaged with new virions and are necessary for proper viral protein function, cDNA synthesis, and cDNA integration into the host genome [22].

The Env glycoprotein, which consists of gp120 and gp41, is also synthesized as a 160kDa glycoprotein precursor protein which requires cleavage into its individual proteins [22]. A signal peptide sequence on gp160 signals for ER trafficking and post-assembly modification and glycosylation. After modification, gp160 is cleaved into gp120 and gp41 by a furin-like protease [22]. From there transmembrane protein gp41 proteins are assembled into Env trimers with gp120 molecules [22].

Two main proteins of interest in relation to lectin inhibition of HIV-1 are gp41 and gp120. The outer viral envelope of HIV consists of phospholipids taken from the host cell, whereas gp41 and gp120, encoded by the env genes of HIV, form the viral envelope spike [23]. Structurally, gp120 trimers associate with GP41 trimers in a non-covalent manner to form the envelope spike [23]. This spike then interacts with the CD4 receptor present on target cells as well as either the CCR5 or CXCR4 co-receptor molecules to initiate cellular infection (Fig. 1.2) [24-27].

HIV Course of Infection

The functional course of viral infection of a susceptible T-cell follows a characteristic pathway. First, gp120 present on the envelope of HIV binds with the CD4 receptor molecule, which normally assists with the activation of T-cells upon interaction with an antigen presenting cell (Fig. 1.2) [24, 28-29]. Upon binding, the core of the gp120 trimer undergoes conformational changes, resulting in greater flexibility and interaction with either the CCR5 or CXCR4 co-receptor, which are necessary for further steps in viral fusion [30-32]. Following

co-receptor engagement, a conformational change occurs in the envelope spike, altering the state of gp41 [33-34]. This conformational change allows the n-terminal domain of gp41 to become exposed and inserted into the cellular membrane [33]. Finally, this insertion induces a final structural change causing the formation of a six-helix bundle, which provides the force necessary for cellular fusion [33-35].

Upon successful cellular fusion, the capsid releases two copies of RNA as well as the accessory molecules necessary for replication – reverse transcriptase, integrase, and viral protease. Reverse transcriptase converts the RNA copies to DNA [22]. Integrase functions to cleave the host DNA, integrating the viral DNA into the host cell's genome [22]. Viral protease serves to cleave precursor polyproteins into their functional units [22].

The mechanisms of productive systemic infection can vary somewhat by point of entry. In HIV-1 transmission following mucosal exposure, cellular binding of the viral particle to a susceptible cell is the first step in the process of HIV infection. It has recently been come to be understood that successful infection often is accomplished by HIV isolates which have more compact variable loops of gp120, with reduced numbers of N-linked glycans [36]. These viral particles infect suboptimally activated memory CD4+ T cells in the genital mucosa [37-39]. Following low level replication, HIV-1 infects fully activated CD4+ T cells, leading to migration of the virus to gut-associated lymphoid tissues where viral replication is further amplified [40-41]. This leads to a high level viremia that establishes

acute infection as well as a depletion of gut-associated T-cells possessing the $\alpha 4\beta 7$ gut homing integrin [36].

Vaginal transmission is the most common route of transmission worldwide, as the majority of HIV-1 infected individuals worldwide are women. It is believed that the cervix, which has a less protective columnar epithelium and is rich in HIV-1 target cells, is a major site for HIV-1 transmission[42-44]. After sexual intercourse, this area is exposed to seminal fluid, allowing contact between virions and susceptible cells.

Receptive anal intercourse provides the greatest probability of mucosal transmission [45-46]. This is likely due to two factors; a fragile layer of columnar epithelium that can be damaged by the virus, and a high level of constitutively activated T lymphocytes in the gut epithelium [45, 47-49]. However, even in the absence of epithelial damage, HIV-1 transmission in the anal mucosa can occur through transcytosis or through infection of dendritic cells [50-51].

During penile transmission occurring during sexual intercourse, the route of infection likely occurs via either the inner foreskin or through the penile urethra [52-53]. The inner foreskin has abundant levels of HIV-1 target cells, including CD4+ T cells, macrophages, and Langerhans cells [52]. Furthermore, the penile urethra also has a population of CD4+ T cells and macrophages [52]. Thus, during sexual intercourse, these surfaces become exposed to infected fluids, exposing vulnerable tissues to potential infection.

GP120 structure and glycosylation

As a protein produced by its eukaryotic host cells, the gp120 protein of HIV is highly glycosylated, with an average of 24 glycosylation sites [54]. Recent studies have shown that the glycosylation state of gp120 consists almost entirely of the high-mannose variety [20]. It is currently hypothesized that this is due to the inability of host editing proteins and α mannosidases to access the glycans effectively, resulting in the inability to modify high mannose glycans into a hybrid or complex form [20].

As with similar proteins, gp120 N-linked glycosylation relies on the signal triplet Asn-X-Ser or Asn-X-Thr for the addition of the carbohydrate chains. However, given the low fidelity of the HIV reverse transcriptase, there can be great diversity in the number of high mannose glycans present on gp120 as the virus evolves to avoid host defense mechanisms. Some studies have shown that an increase in potential N-linked glycosylation sites can result in increased viral fitness by reducing sensitivity to host produced neutralizing antibodies by obscuring binding sites recognized by antibodies [55].

However, other studies have shown that decreases in glycosylation sites may also play a role in viral fitness and infectivity. Studies of sequence data has demonstrated that viral particles in a newly infected host have fewer glycosylation sites as well as shorter variable loops [56-57]. These changes are believed to facilitate the binding of the virus to the host receptor cells without the interference by the carbohydrate chain additions. However, as the virus begins replicating and is placed under neutralizing antibody pressure, an increase in

glycosylation sites is observed. Accordingly, additions of glycosylation sites in the gp120 may promote viral fitness in successive replication cycles by allowing the virus to evade neutralizing antibodies by denying them access to previously recognized epitopes.

Antiviral treatments

Many different pharmacological strategies and drugs are currently in use for the treatment of HIV. These drugs include non-nucleoside reverse transcriptase inhibitors, nucleoside reverse transcriptase inhibitors, protease inhibitors, integrase inhibitors, and fusion inhibitors. These therapies have greatly increased the ability of an HIV infected individual to live close to a normal life span. Prior to the advent of Highly Active Anti-Retroviral Therapy (HAART), the expected survival span of an individual infected with HIV was 5 to 10 years. Today, the life expectancy of a 20 year old starting antiretroviral therapy is an additional 49 years [58]. The goal of HAART is to preserve immune function, extend survival time, as well as suppress viral load to undetectable levels.

However, the complete elimination of HIV in those already infected seems unlikely, if not impossible, due to the establishment of viral reservoirs within the body which maintain a base level of infection, even while viral loads are deemed undetectable. It is theorized that these viral reservoirs are the result of a latent infection of long lived cells, or a suppressed but continual low level viremia in which active cell to cell transmission continues to occur, or a combination of both of those factors [59-63]. Accordingly, an agent that could further prevent cell-to-cell transmission of HIV, and thus assist in reducing or eliminating viral

reservoirs, would be an attractive complementary treatment to those whose viral loads are suppressed to undetectable levels.

Entry Inhibitors

Among some of the newest agents currently being investigated as a treatment of these viruses are entry inhibitors that can prevent viral fusion with its target cell at various phases of the viral entry process. Entry inhibitors can act in a number of ways, including presenting a physical barrier to viral fusion by binding to the virus to prevent infection or by altering the cellular receptors necessary for viral infection [13, 64]. Entry inhibitors can currently target a number of proteins on either the virus or the cell. These targets include gp120 or gp41 of HIV virions, the CD4 receptor present on T-cells, or the CCR5 or CXCR4 co-receptors present on CD4 cells.

T20, or Enfuvirtide, is an injectible peptide fusion inhibitor [65]. Enfuvirtide is commonly used as part of a combination therapy when other therapies have failed. Enfuvirtide acts by binding to gp41, preventing conformational changes that are necessary for successful cellular infection (Fig. 1.2D) [34]. As a 36 amino acid peptide, it mimics the HR2 fragment of gp41, and binds to the HR1 region of gp41 [66-67]. Binding to the H1 region thus blocks formation of the six helix bundle, the primary driving force for the final steps of cellular fusion process [34]. In 2003, enfuvirtide was approved for treatment of HIV infection, due to virological benefits seen when added as an adjunct antiretroviral regimen [68].

Maraviroc is a small molecule, CCR5 co-receptor antagonist, which is also used as an entry inhibitor in the treatment of HIV-1 [69-71]. Maraviroc

allosterically binds to the transmembrane cavity of the CCR5 co-receptor, thus blocking its interaction with gp120 after gp120 has bound to the CD4 receptor (Fig. 1.2C) [72]. This prevents subsequent binding steps and conformational changes necessary for viral fusion with the cell.

Ibalizumab is a CD4-targeting antibody that is currently being examined as an entry inhibitor [73-75]. While non-immunosuppressive, Ibalizumab binds the CD4 molecule present on T-cells in the D2 region of the receptor (Fig. 1.2A) [76-77]. This binding prevents conformational changes in the CD4 receptor necessary for later steps in cellular infection. However, it does not interfere with either the binding of MHC II molecules or the gp120 to the receptor, and thus does not interfere with normal immune function [76-78].

One class of potential entry inhibitors are a subset of lectins, carbohydrate binding agents. Generally, lectins are highly specific sugar binding proteins which can agglutinate cells or precipitate conjugated sugars. Lectins can serve a variety of purposes in plant and animal cells. In animals, they can serve to regulate cell adhesion and by recognizing carbohydrates exclusively present on pathogens. For example, mannose binding lectin is a serum protein which plays a role in innate immunity by binding to pathogens, resulting in activation of the complement system or opsonization of the pathogen [83].

Antiviral lectins are a subset of lectins which bind to the envelope glycans of many viruses, including HIV and HCV [7]. This subset includes Concanavalin A, Cyanovirin, and Actinohivin [12, 79-80]. While different lectins have different carbohydrate targets, it is believed that antiviral lectins effective against HIV

infection inhibit viral transmission by selectively binding to the N-linked high-mannose glycans present on the surface of the trimeric gp120 spike, thus preventing cellular fusion (Fig. 1.2B) [7]. It has also been theorized that cross-linking and aggregation of viral particles may also be an additional and equally vital mechanism of viral inhibition [81].

Despite their promise as potential neutralizing agents for HIV and HCV, lectin treatment can present a challenge. Aside from potential side effects due to mechanism of drug action, the presence of proteinaceous drugs can induce allergic reactions and anaphylaxis. As foreign proteins, there is no opportunity for central tolerance to their sequences to develop within immature T and B cells. Accordingly, exposure to the protein can activate T and B cells, initiating an immune reaction [82]. However, immune reactions can vary. Neutralizing antibodies can also be generated which effectively bind the protein and facilitate its degradation [82]. However, it is also possible that type I immediate hypersensitivity reactions can be initiated which result in anaphylaxis [82]. Anaphylaxis is a potentially deadly reaction to immunogens wherein mast cells are degranulated by the binding of IgE [82]. Multivalent binding of IgE to antigen results in cross linking of FcRe, which activates degranulation [82]. This degranulation results in the release of large amounts of histamine and TNF- α [82].

Anaphylaxis has been observed in a number of proteinaceous drug treatments. These drugs include Omalizumab, a monoclonal antibody treatment for asthma, alpha galactosidase A for the treatment of Fabry's disease,

and Rituximab for the treatment of leukemias and autoimmune disorders [83-86]. Fortunately, interventions can be used to delay and mitigate reactions to foreign proteins. For example, treatment with methotrexate can delay immune response to α -Galactosidase A therapy [87]. By depressing certain immune function, the numbers of activated and replicating immune cells is decreased, resulting in a decrease in potential production of antibodies. Nonetheless, as effective protein therapies are employed, a full understanding of the potential immunological consequences of drug administration will be valuable in devising strategies to avoid such immune responses.

Griffithsin Structure and Mechanism of action

GRFT is a carbohydrate binding agent with high affinity for N-linked high mannose glycans [13-14]. In solution, GRFT forms a domain swapped homodimer with a total of 6 mannose binding sites, as determined by X-ray crystallography of GRFT at 1.3Å resolution [88-89]. Structural complexes of GRFT with both mannose and N-acetylglucosamine have defined locations of 3 virtually identical carbohydrate binding sites on each monomer which use a highly conserved GGSGG motif found in the loops of the protein [90]. This sequence, as well as a dimeric domain swap forming the third binding pocket on each side, provides amide groups which form the ligand binding sites. Upon dimerization, GRFT's binding sites form an almost equilateral triangle on the edge of the protein, creating two opposing surfaces for mannose binding [88].

GRFT's anti-HIV inhibitory capacity is mediated through its binding to the high-mannose glycans present on the gp120 spike of HIV [14]. This binding

interaction thus becomes a barrier to infection by preventing interaction between the viral gp120 and the CD4 molecule of its target cells. Supporting this theory is the fact that lectin-resistant isolates of HIV have been generated in the laboratory by placing HIV under increasing concentrations of GRFT over successive passages [4]. A genomic analysis of the envelope glycoproteins of these isolates reveals that a number of glycosylation sites in the resistant viruses were deleted, thus decreasing the number of potential binding sites for lectin activity.

To determine whether systemic effects of GRFT are the result of the active site of GRFT or simply by the presence of foreign proteins, we have developed a mutated form of the drug, GRFT^{lec-}, in which the carbohydrate binding sites have been ablated by amino acid substitution (a substitution of asparagine for aspartic acid residues in the binding pockets). While structurally similar to mannose-binding GRFT in structure and sequence, this mutated form does not bind high mannose glycans and demonstrates no antiviral activity in pseudovirus challenges.

In order for GRFT to be a viable systemic antiviral treatment, it must be able to be efficiently and economically produced, maintained in blood serum at safe and therapeutic levels, and retain its anti-viral activity in the systemic circulation. Prior work has demonstrated that GRFT is able to be efficiently and economically produced in large quantities [91-92]. Additionally, prior studies have demonstrated GRFT's weak immunogenicity and low induction of inflammatory cytokines and chemokines [13, 92]. However, little study has yet been conducted into the systemic tolerability of GRFT or the retention of its anti-

viral activities *in vivo*. Furthermore, given that HIV is known to acquire drug resistance when placed under drug pressure, insight is needed into the molecular interactions that result in GRFT-resistant isolates.

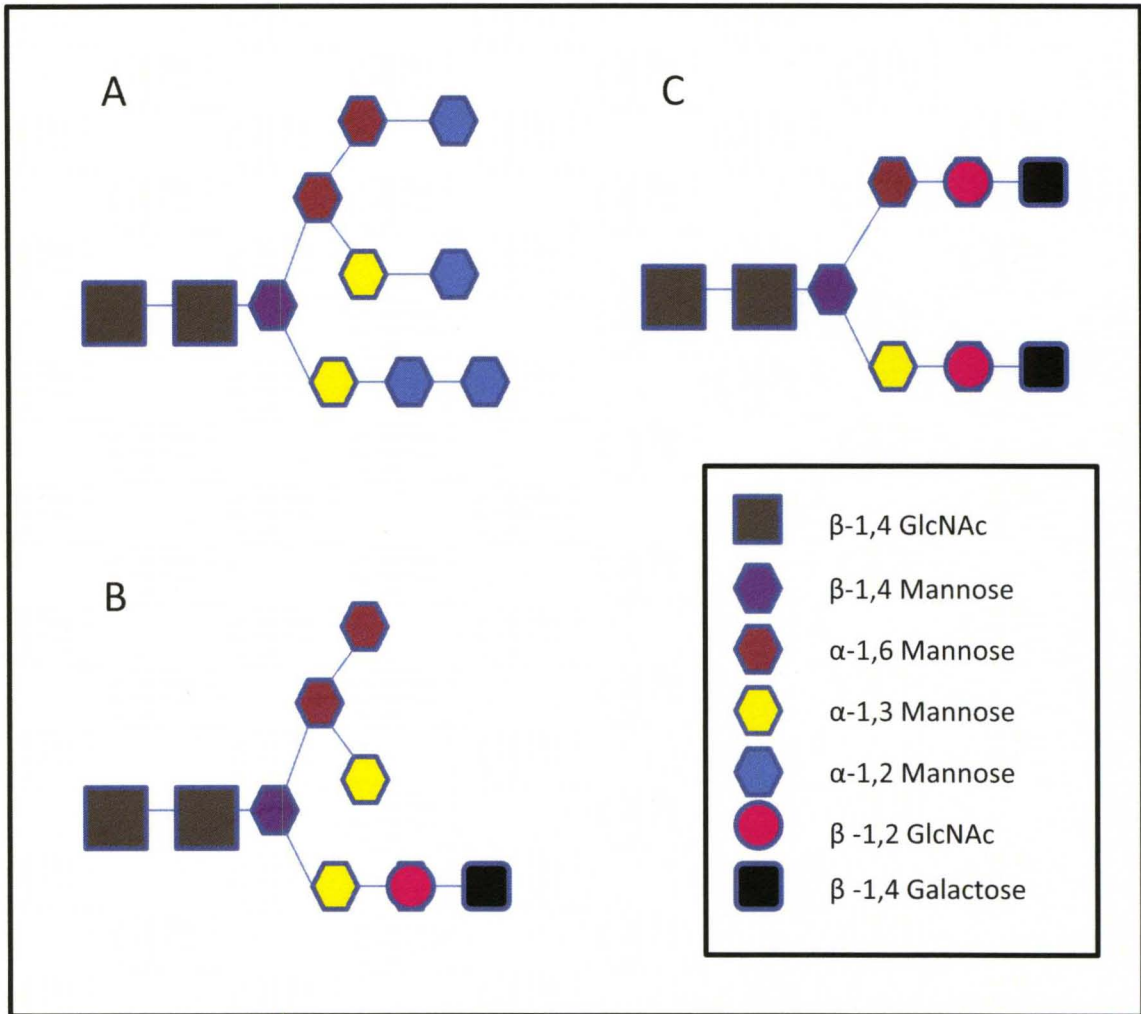


Figure 1.1. N-linked glycans - structural arrangement of subtypes. Schematic depicting examples of different types of N-linked glycans. High Mannose glycans (A) present exclusively mannose termini. Hybrid glycans (B) present a mixture of mannose termini and GlcNAc termini. Complex glycans (C) are devoid of mannose termini.

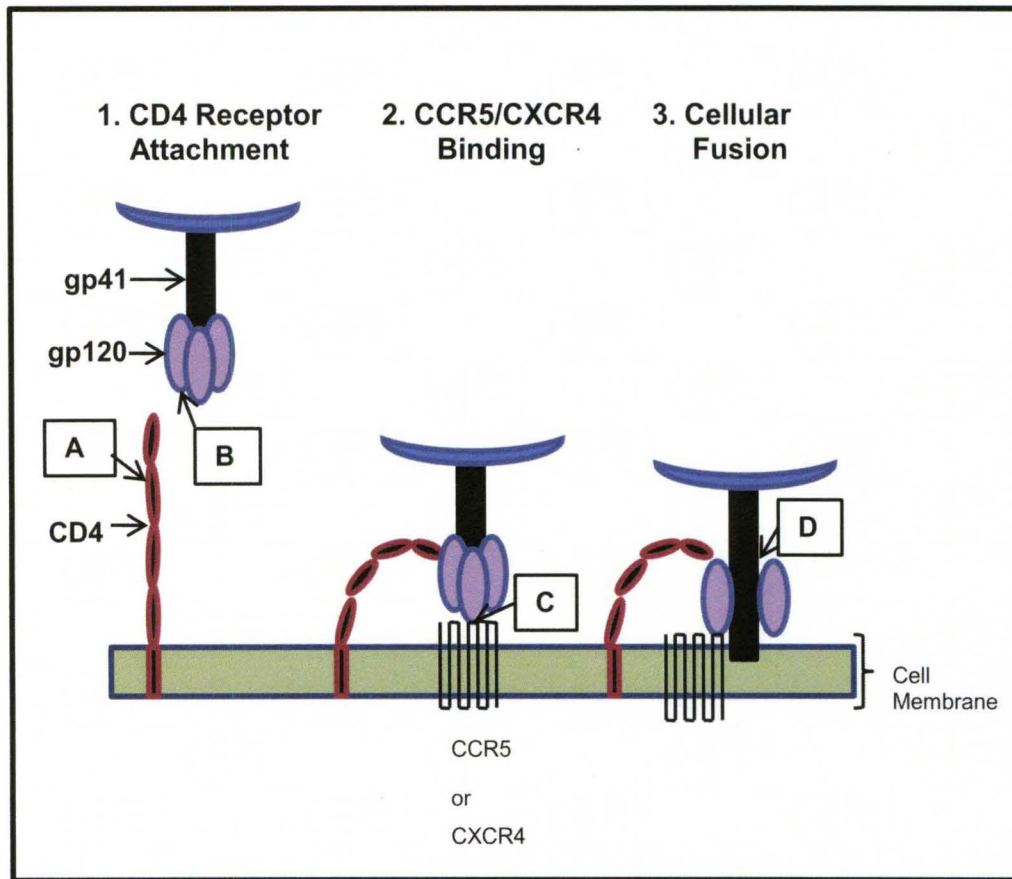


Figure 1.2. Steps of HIV-1 cellular entry highlighting sites of potential therapeutic interventions. The above schematic demonstrates the steps of HIV-1 entry relevant to different entry inhibitors including CD4 attachment, co-receptor binding, and cellular fusion. Potential therapeutic intervention points include: (A) Ibalizumab binding site on the CD4 molecule to prevent CD4 conformational changes necessary for co-receptor binding, (B) lectin binding sites for glycans present on gp120 to prevent proper CD4 interactions, (C) Maraviroc (CCR5 antagonist) binding site to prevent gp120/co-receptor interaction, and (D) Enfuvirtide (T20) binding site to prevent conformational changes in gp41 necessary for the final stages of cellular fusion.

CHAPTER 2

ASSESS GRFT'S SHORT TERM SYSTEMIC TOLERABILITY, ANTI-VIRAL ACTIVITY, AND SERUM PERSISTENCE IN THE ABSENCE OF AN ANTIBODY RESPONSE

INTRODUCTION

In this Chapter we will examine the systemic effects that subcutaneously injected GRFT has upon the systemic physiology of female guinea pigs (*Cavia porcellus*). Given GRFT's demonstrated ability to block cell to cell transfer of HIV-1, it is important to fully investigate any short term toxicological impacts that GRFT has on a living system's physiology. Due to an inherently low background HIV neutralizing activity in serum and blood, guinea pigs were chosen for the animal model in this study so as to allow for full evaluation of GRFT's continued neutralizing capacity after systemic introduction.

Given that the introduction of a foreign protein into a living system will expose said protein to a vast number of proteases and potential degradatory pathways, it was important to ascertain whether GRFT would: 1. maintain its stability in serum; 2. maintain its anti-viral activity in an environment in which

endogenous high mannose binding may occur; and 3. distribute into particular organs or tissues.

For the experiments described in this chapter, GRFT, GRFT^{lec-}, or PBS was injected subcutaneously into guinea pigs for a period of ten days. Drug effects on Complete Blood Counts (CBC's), normalized organ weights, body weight, and select serum chemistries were monitored for any changes in experimental groups relative to PBS-treated controls. Additionally, histological analysis of kidneys, spleens, livers, and vaginas was carried out on all animals to document treatment associated pathologies as well as to determine whether pathologies were due to protein presence or drug action. Finally, hemagglutination assays were conducted to evaluate whether GRFT, as a lectin, has the ability to cause erythrocyte aggregation. Potential aggregation of erythrocytes could cause potential increases in red blood cell turnover, as well as possibly make GRFT unable to be used in systemic circulation.

MATERIALS AND METHODS

Twenty-six (26) female Hartley guinea pigs (Charles River), ranging from 6-8 weeks of age were chosen as the animal model given their low anti-HIV neutralizing background in blood and serum. Six groups were formed, consisting of 6 PBS treated animals (Groups 1a and 1b), 10 GRFT-treated animals (Groups 2a and 2b) and 10 GRFT^{lec-} treated animals (Groups 3a and 3b).

Injection and Dosage

GRFT, manufactured by Kentucky Bioprocessing, LLC, was diluted in Phosphate Buffered Saline (PBS, pH 7.4) to achieve a final concentration of 10mg/ml. GRFT^{lec-}, already at 9.5mg/ml, required no dilution before administration. Subcutaneous injections of the appropriate drug solution or vehicle (PBS) were conducted daily for a period of 10 days. Control group members were injected with 1ml/kg/day PBS, while animals from test groups 2 and 3 received doses of 10mg/kg/day of GRFT or GRFT^{lec-}, respectively. For dosage determination and adjustment, all animals were weighed on days one and five.

Sample collection

Group members from 1a, 2a, and 3a were weighed and euthanized twenty four (24) hours after last treatment. All remaining group members were weighed and euthanized 96 hours later. Euthanizations via cardiac puncture exsanguination were performed under isoflurane anesthesia, followed by thoracotomy. Vaginal lavage samples for Groups 1a, 1b, 2a, and 2b were taken

via pipette using PBS prepared with 1 x Protease Arrest and EDTA (G Biosciences) to prevent proteolytic degradation of GRFT. Kidneys, livers, spleens, and vaginas were excised, weighed, and fixed in 10% formalin for 48-72 hours. After fixation, organs were placed in 70% ethanol and sent for slide preparation, hematoxilin & eosin staining, and histological analysis.

Measurement of GRFT Concentrations

Serum was collected from blood samples by centrifugation and concentrations of active GRFT were determined using a GP120 sandwich ELISA. Briefly, 96-well Maxisorp plates were coated with 100 μ l gp120 diluted in PBS, at a concentration of 250 ng/ml. After overnight incubation at 4°C, and subsequent blocking of the plate wells with 3% BSA in 1xPBS-T, serum samples were diluted (1:10) in blocking buffer and incubated in the 96-well plate at room temperature for one (1) hour. After washing in PBS-T, polyclonal rabbit anti-GRFT primary antibody (1:25000 dilution in blocking buffer) was incubated for 1-2 hours. After a second cycle of PBS-T washes, wells were incubated with a HRP-conjugated goat anti-rabbit secondary antibody (1:10000 dilution in blocking buffer) for one hour. Following the one-hour incubation, wells were washed, and 100 μ l of SureBlue TMB Microwell Peroxidase substrate was added to each well and developed in the dark for 10 minutes. The addition of 100 μ l of 1N sulfuric acid was used to stop the reaction. Absorbance readings at 450 nm and 570 nm were measured using a BioTek Synergy HT plate reader.

Concentrations of GRFT^{lec-}

GRFT^{lec-} concentrations were not amenable to detection via gp120 sandwich ELISA given the inability of GRFT^{lec-} to bind to gp120. Accordingly, we attempted to detect GRFT^{lec-} presence by SDS PAGE and Western blot. Serum drawn from GRFT-treated guinea pigs and serum drawn from GRFT^{lec-}-treated guinea pigs were diluted 1:1 in sample buffer and separated by SDS PAGE on an anyKD readygel (Biorad) for 20 minutes at a constant 200 volts. Transfer to PVDF membrane was accomplished using a transfer buffer of 10% Methanol, 10mM N-cyclohexyl-3-aminopropanesulfonic acid (CAPS) buffer. Transfer was carried out at 200v for 25 minutes. After transfer to PVDF, the membrane was blocked using a blocking buffer consisting of 5% non fat dry milk (NFDM) in PBS. GRFT and GRFT^{lec-} presence was evaluated by incubating the membrane in a rabbit anti-GRFT primary antibody (diluted 1:25000 in blocking buffer) for one hour at room temperature. Following primary antibody incubation and rinsing in PBS-T, the membrane was incubated in a goat anti-rabbit HRP-conjugated secondary antibody (diluted 1:10000 in blocking buffer) for one hour at room temperature. The membrane was washed in PBS-T and chemiluminescence was detected by exposure of the PVDF membrane to X-ray film after addition of HRP substrate.

Anti-HIV Activity

The anti-HIV activities of serum and vaginal lavage samples were measured by our collaborator at Duke University, David Montefiori using a pseudovirus neutralization assay. Antiviral activity was measured as a reduction

in luciferase reporter gene expression as previously described[93]. ID₅₀ values, which represent antiviral activity, were reported as sample dilutions at which relative luminescence units (RLUs) were reduced 50% compared to virus control wells containing no serum or vaginal lavage sample. Virus stocks of molecularly cloned Env-pseudovirus of Du156.16 were prepared by transfection of 293T cells and were titrated in TZM-bl cells as previously described. [93]

CBC and Serum Chemistry

At sacrifice, blood drawn via cardiac puncture exsanguination was aliquotted into vials containing EDTA for complete blood count (CBC) analysis. A complete CBC profile for each guinea pig in the control and GRFT-treated groups was generated. Briefly, 20 µl of whole blood was loaded into a Hemavet 950FS and run according to manufacturer's directions. The CBC profile included examination of the following: White blood cells (WBC), Neutrophils(Ne), Lymphocytes (Ly), Monocytes (Mo), Eosinophils (EO), Basophils (Ba), Red Blood Cells (RBC), Hemoglobin (Hb), Hematocrit (HCT), Mean Corpuscular Volume (MCV), Mean Corpuscular Hemoglobin (MCH), Mean Corpuscular Hemoglobin Concentration (MCHC), Red blood cell distribution width (RDW), Platelet and Mean Platelet volume (MPV). Based upon the results of a pilot study on the effects of GRFT on guinea pig serum chemistries, three serum chemistry profiles were analyzed: serum albumin (Alb), alkaline phosphatase (ALKP), and amylase (Amy). Serum samples from all treated animals was obtained as described previously and tested for the selected chemistry values.

Immunofluorescent Imaging

GRFT presence in unstained, formalin fixed tissue slide was visualized by immunofluorescent detection. Organ slides were deparaffinized and hydrated by duplicate and successive 10 minute incubations in HistoClear, 100% ethanol, and 95% ethanol. Slides were then subjected to antigen retrieval by immersion in 1mM sodium citrate buffer and high pressure heating using a 2100 Retriever antigen retriever. Following a 10 minute PBS wash with agitation, slides were blocked with 5% goat serum (v/v) in PBS for 15 minutes. Slides were then incubated with polyclonal rabbit anti-GRFT primary antibodies at 1:100 dilution in blocking buffer for one (1) hour. After washing in PBS, slides were incubated for one hour with a FITC-conjugated goat anti-rabbit secondary antibody at a 1:500 dilution. After final incubation, slides were washed twice in PBS for 10 minutes per wash. Slides were cover-slipped with Prolong Gold Anti-fade reagent with DAPI . Slides were then imaged at 200x magnification using an Olympus CKX41 microscope and the appropriate fluorescence filter.

Hemagglutination

Hemagglutination activity of GRFT was evaluated. To test GRFT's hemagglutination activity guinea pig erythrocytes (Innovative Research) were washed with PBS to remove cell debris. Cell suspensions were spun down at 1000 x g for one minute and resuspended at a final cell concentration of 1-2% in PBS containing 3 g/L BSA and 1 g/L sodium azide. Serial dilutions of either Phytohemagglutinin (PHA) (positive control) or GRFT were mixed with an equal volume of erythrocytes in a 96 well round bottom plate (total 100 μ L/well) and

incubated for 1 hr at room temperature, followed by overnight incubation at 4°C. Plates were then allowed to dry. Hemagglutination activity was determined by visual examination of erythrocyte aggregation or dissemination versus controls, with hemagglutination activity indicated by dissemination of blood cells in the entire well as opposed to collection of blood cells into a single point.

Statistical Analysis

Statistical analysis was conducted using the Graph Pad Prism 5 program. Groups were split between time points of day 11 (24 hour) results and day 15 (120 hour) results, reflecting date of euthanization. ANOVA was performed for weight changes, organ weight differences, and serum chemistries between time-matched groups. For the analysis of CBC data, for which GRFT^{lec-} data was not collected, t-tests between time-matched Control and GRFT-treated groups were used. A p-value of <0.05 was deemed significant.

RESULTS

Animal Morbidity and Mortality Observations

No animals were lost during the treatment period. No unusual behavior during the treatment period was noted.

GRFT Serum Blood concentration

GRFT-treated animal sera contained measurable concentrations of GRFT 24 and 120 hours after last treatment. GRFT concentrations detected in serum via a GP120-binding ELISA were plotted against their applicable test group (Fig. 2.1). PBS-treated control groups 1a and 1b showed no GRFT presence. Day 11-group 2a displayed an average GRFT concentration of 36 nM. Day 15-group 2b displayed an average serum GRFT concentration of 11.36 nM.

GRFT^{lec-} Serum Blood concentrations

GRFT^{lec-} was not detected by Western blot in serum from groups 3a and 3b (Img. 2.1). Serum from groups 2a and 2b were run in parallel, with GRFT detected in those samples. Purified GRFT^{lec-} was run as a control to ensure that the rabbit polyclonal antibody could detect the mutated form of GRFT. As expected, a band was observed at 12.7 kDa.

GRFT Vaginal Wash Concentrations

Concentrations of GRFT in vaginal lavage samples were determined by gp120-binding ELISA (Fig. 2.1). GRFT-treated animals displayed measurable concentrations of GRFT in vaginal wash samples at both 24 and 120 hours after last systemic administration, however GRFT was not detected in vaginal lavage samples from PBS-treated animals. Vaginal washes from Group 2a animals

displayed an average detectible GRFT concentration of approximately 9 nM.

Furthermore, vaginal washes from Group 2b animals continued to display

detectible GRFT concentrations of 2 nM.

Anti-HIV Activity

Antiviral activity was quantified using serum and vaginal wash samples of animals treated with GRFT. HIV env-pseudovirus neutralization assays revealed that GRFT retains its anti-HIV activity while in serum. Anti-viral activity was plotted against the group from which serum was collected (Fig. 2.2). ID₅₀ values, representing anti-viral activity, were reported as the sample dilution at which relative luminescence units (RLUs) were reduced 50% compared to virus control wells containing no test sample. Sera from PBS-treated control groups displayed a mean neutralization activity of less than 20. Sera from GRFT-treated animals in Group 2a displayed a mean HIV neutralization capacity of 3277. Serum samples from GRFT-treated animals in Group 2b displayed an average neutralization activity value of 576.

Vaginal wash samples also displayed measureable anti-HIV activity, however at much lower levels than those found in serum. Vaginal wash samples from Group 2a were deemed to have a mean neutralization capacity of approximately 70, whereas samples from Group 2b possessed a mean neutralization capacity of approximately 40.

Guinea Pig CBCs

No significant differences were observed on either day 11 or day 15 in the numbers of the following categories: White Blood Cells, Neutrophils, Lymphocytes, Monocytes, Eosinophils, Basophils, Red Blood Cells, Hemoglobin, Hematocrit, Mean Corpuscular Hemoglobin, Mean Corpuscular Hemoglobin Concentration, Platelets, or Mean Platelet Volume (Table 2.1). However, Group 2b red blood cell distribution width (RDW) and Mean Corpuscular Volume (MCV) values were significantly different. Despite the statistically significant difference in RDW values, all values for RDW were within normal physiological range for guinea pigs, according to normal ranges for guinea pigs coded within the Hemavet 950FS programming.

Alkaline Phosphatase, Amylase, and Albumin.

Analysis of serum chemistries revealed significant differences in serum albumin and amylase levels on day 15 (120 hours post treatment). Bonferroni post test comparisons between treatment groups vs. controls revealed that the differences seen in ANOVA analysis were attributable to differences observable in GRFT^{lec-} treated groups, which were significantly lower than controls.

Animal weight gain

Analysis of animal weight gains during treatment revealed differences in percentage weight gain between groups. Animals in groups 2a (GRFT-treated) and 3a and 3b (GRFT^{lec-}-treated) experienced significantly less weight gain than time-matched PBS controls. Animal percentage weight gain during treatment was calculated and separated by sacrifice day and test group (Fig. 2.3). On day

11, Group 1a control animals had experienced substantially greater weight gain than both GRFT and GRFT^{lec-}-treated groups (groups 2a and 3a). Furthermore, GRFT^{lec-}-treated animals in Group 5 continued to display significantly less weight gain in comparison to PBS-control group 1b. However, group 2b no longer displayed a statistically significant difference when compared against controls when analyzed by Bonferroni post hoc test.

Organ weights

Liver, kidney, and spleen weights at time of sacrifice were analyzed for significant change in relation to total body weight. Average organ weight- to-body weight percentages were plotted against test groups (Fig. 2.4). Liver weights showed no significant difference on either day 11 or day 15. Results for kidney weight were mixed, with no difference observed at day 11. However on day 15 there was a significant difference amongst groups observed when analyzed by two-way ANOVA. A Bonferroni post test between test groups vs. control was conducted, showing a significant difference control and GRFT^{lec-}-treated groups. Spleen weight difference results were also mixed, with no significant difference observed at Day 11. However, on day 15, GRFT-treated groups displayed a statistically significant greater spleen to body weight ratio when analyzed by ANOVA and Bonferroni post test.

Organ Histopathology and Imaging

Although there were diverse pathologies observed among all treatment groups, no pathologies related to GRFT treatment were observed. Among all treatment groups, notable pathologies included chronic pyelitis in the kidneys,

extramedullary hematopoiesis localized in the spleen, and a minimal or mild chronic portal or periportal hepatitis in the livers.

Immunofluorescent Imaging

Immunofluorescent imaging of organ sections revealed a strong presence of GRFT in GRFT-treated animals both 11 days and 15 days after treatment in the kidneys and spleen (Image 2.1). GRFT appeared to be most concentrated in the spleen, with presence also being observable in the liver, kidney, and vaginal tissue 120 hour post treatment. GRFT^{lec-} was not detectable in any organ tissue tested.

Hemagglutination activity

GRFT's hemagglutination activity in guinea pig blood was analyzed. Visual inspection of wells containing PHA, PBS, and GRFT were compared (Fig. 2.2). As expected, PBS did not show any hemagglutination activity. PHA, a lectin with known activity, demonstrated hemagglutination activity in the 0.5 mg/ml (0.3 μ M) to 10 μ g/ml (78.1 nM) range. Comparisons between wells demonstrated that GRFT possesses hemagglutination activity in guinea pig erythrocytes in the 1mg/ml (41 μ M) to 100 μ g/ml (4.1 μ M) range. At concentrations below 100 μ g/ml, GRFT did not appear to have any significant impact upon erythrocyte agglutination.

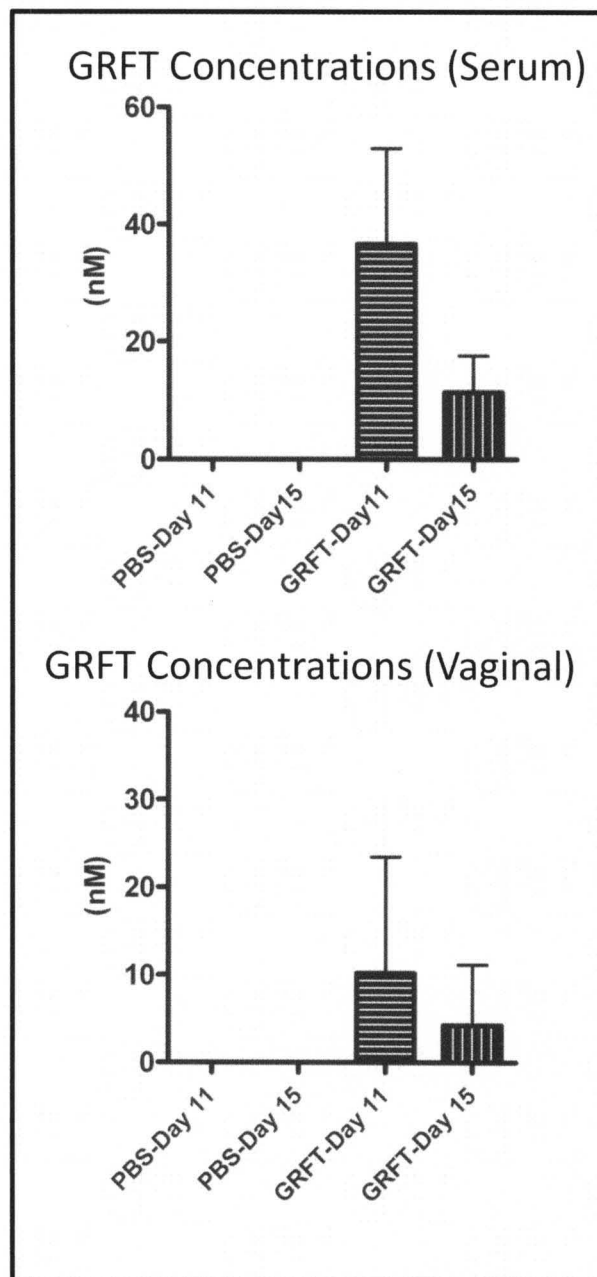


Figure 2.1. Concentrations of GRFT in serum and vaginal washes of guinea pigs treated with GRFT or PBS. Serum and vaginal washes from PBS and GRFT-treated Guinea Pigs was analyzed for GRFT presence. Nanomolar concentrations of GRFT were detectable in both serum and vaginal wash samples at 120 hours after last administration. Bars indicate mean concentrations with standard deviation.

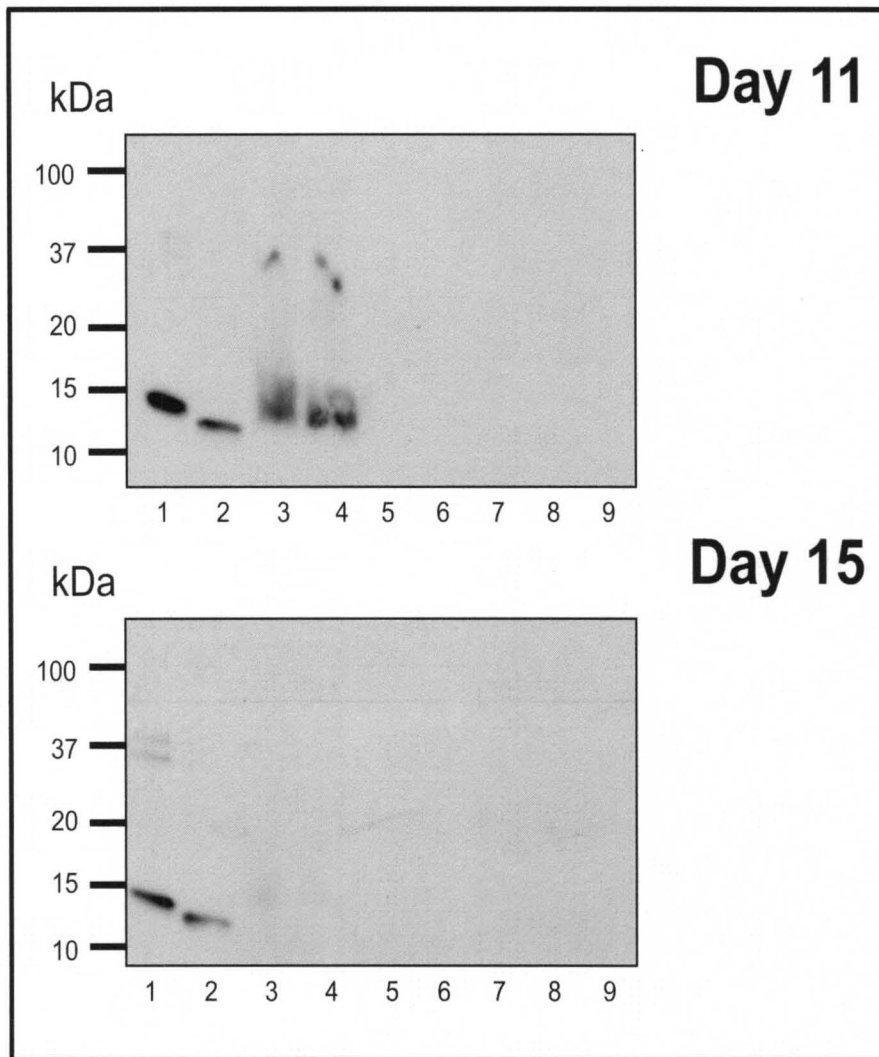


Image 2.1. Western blot of guinea pig serum to determine persistence of GRFT^{lec-}. Serum from GRFT-treated and GRFT^{lec-} treated guinea pigs was diluted in running buffer and examined for GRFT or GRFT^{lec-} presence. At both 24 and 120 hours post cessation of treatment, GRFT was detectible in serum. However, at no time point examined was GRFT^{lec-} detectible. From left, GRFT, GRFT^{lec-}, and two GRFT-treated animal serum samples. Serum from GRFT^{lec-} treated animals was run in lanes 5-9.

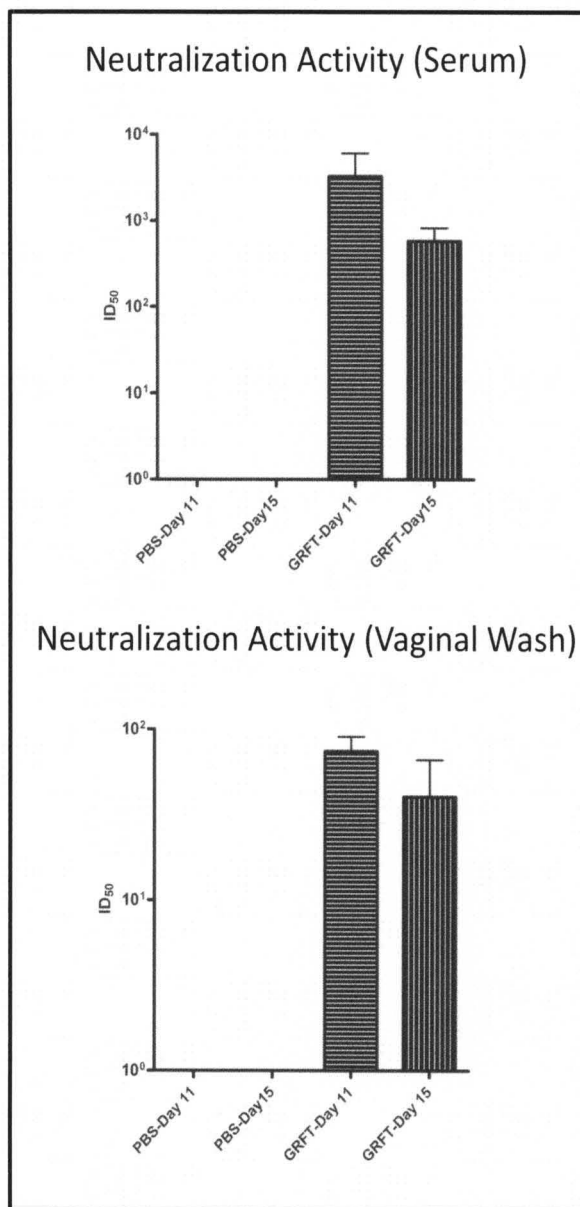


Figure 2.2. Analysis of HIV neutralization activity of guinea pig serum and vaginal wash samples. HIV pseudovirus neutralization was used to test samples. Numbers represent test sample dilution required to reduce luminescence to 50% of test wells containing no serum or vaginal wash sample. Dilutions under 20 were deemed to be non-neutralizing. Bars indicate mean concentrations and standard deviation.

CBC Category	Day 11					Day 15				
	Group 1a		Group 2a		Sig.	Group 1b		Group 2b		Sig.
	N=3	Std.	N=5	Std.		N=3	Std.	N=5	Std.	
WBC	4.92	2.43	2.15	0.23	ns	4.35	1.28	2.9	1.36	ns
NE	2.3	1.46	0.96	0.13	ns	1.67	0.45	1.01	0.42	ns
LY	2.49	1.11	1.14	0.28	ns	2.6	0.89	1.82	0.99	ns
MO	0.09	0.1	0.03	0.03	ns	0.07	0.03	0.06	0.04	ns
EO	0.03	0.02	0.02	0.01	ns	0.02	0.02	0.01	0.02	ns
BA	0	0.01	0	0	ns	0	0	0	0	ns
RBC	4.3	0.06	4.12	0.18	ns	4.75	0.21	4.37	0.22	ns
Hb	12.23	0.64	11.64	0.46	ns	13.1	0.46	12.22	0.61	ns
HCT	38.3	2.31	36.12	1.47	ns	41.57	1.76	39.52	1.94	ns
MCV	88.97	4.73	87.58	1.29	ns	87.53	1.7	90.4	0.52	*
MCH	28.43	1.33	28.26	1.52	ns	27.63	0.61	27.96	1.04	ns
MCHC	31.97	0.25	32.26	1.33	ns	31.5	0.26	30.94	1.11	ns
RDW	13.83	1.43	12.92	0.7	ns	14.13	0.29	12.66	0.7	*
PLT	595.33	54.31	628.6	44.77	ns	677.33	11.93	659	34.26	ns
MPV	4.4	1.14	3.92	0.23	ns	3.57	0.12	3.84	0.24	ns
Normal CBC Values										
WBC	NE	LY	MO	EO	BA	RBC	Hb	HCT	MCV	MCH
6.0-14.0	0.4-6.7	1.9-11.1	0.0-0.7	0.0-1.0	0.0-0.1	4.4-6.0	11.0-15.0	37.0-48.0	77.5-88.5	22.0-28.0
			MCHC	RDW	PLT	MPV				
			28.9-32.0	2.4-27.0	380-650	5.0-20.0				

Table 2.1. CBC values for PBS and GRFT-treated guinea pigs. Whole blood samples were analyzed. Values are group averages with standard deviation. Two significant changes were observable in GRFT treated animals are denoted by (*).

	Day 11							Day 15						
	Grp. 1a N=3	Std.	Grp. 2a N=5	Std.	Grp. 3a N=5	Std.	Sig	Grp. 1b N=3	St d.	Grp. 2b N=5	Std.	Grp. 3b N=5	Std.	Sig
ALB	2.0	2.2	2.3	0.2	2.0	0.3	ns	2.4	0.2	2.2	0.3	1.9	0.2	*
ALK	166.3	36.7	249.2	61.9	207.6	39	ns	146.7	76	255.6	70	217.8	50.0	Ns
AMY	702.7	123	883.0	201	657.4	75	ns	817.3	81	820.2	141	629.6	75.8	*

Table 2.2. Select serum chemistry values for PBS, GRFT-treated, and GRFT^{lec-} treated guinea pigs. Serum samples were analyzed for the above chemistry values. Significant changes were observed in serum albumin and amylase levels in GRFT^{lec-} treated animals, with those animals displaying chemistry values lower than controls.

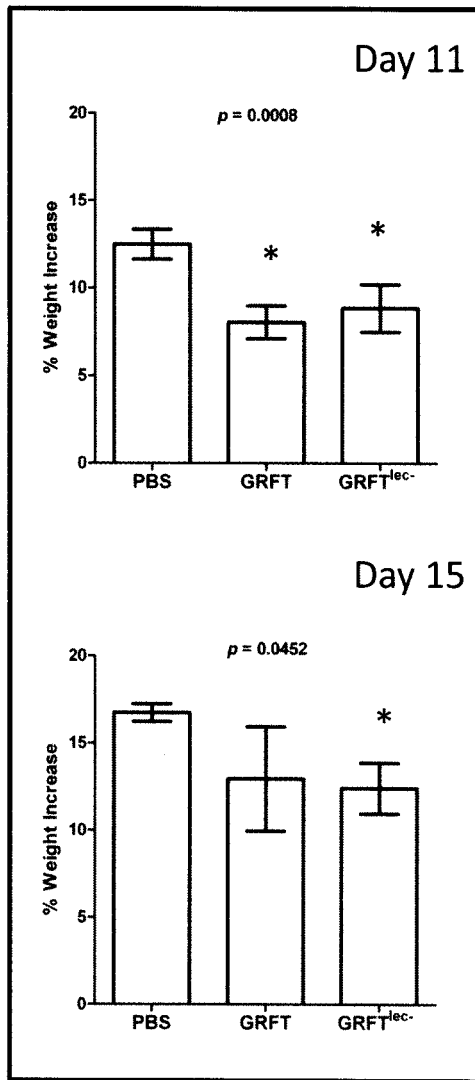


Figure 2.3. Mean whole body weight increases during treatment with PBS, GRFT, or GRFT^{lec-}. GRFT, GRFT^{lec-}, and PBS treated animals were weighed at initiation of treatment and at sacrifice. Average percentage weight gain was analyzed. Significantly less weight gain was seen in GRFT and GRFT^{lec-} treated groups at 24 hours after treatment completion (day 11). GRFT^{lec-} treated animals continued to display significantly less weight gain at 120 hours after treatment completion (day 15). Bars indicate standard deviation, with significance denoted by (*).

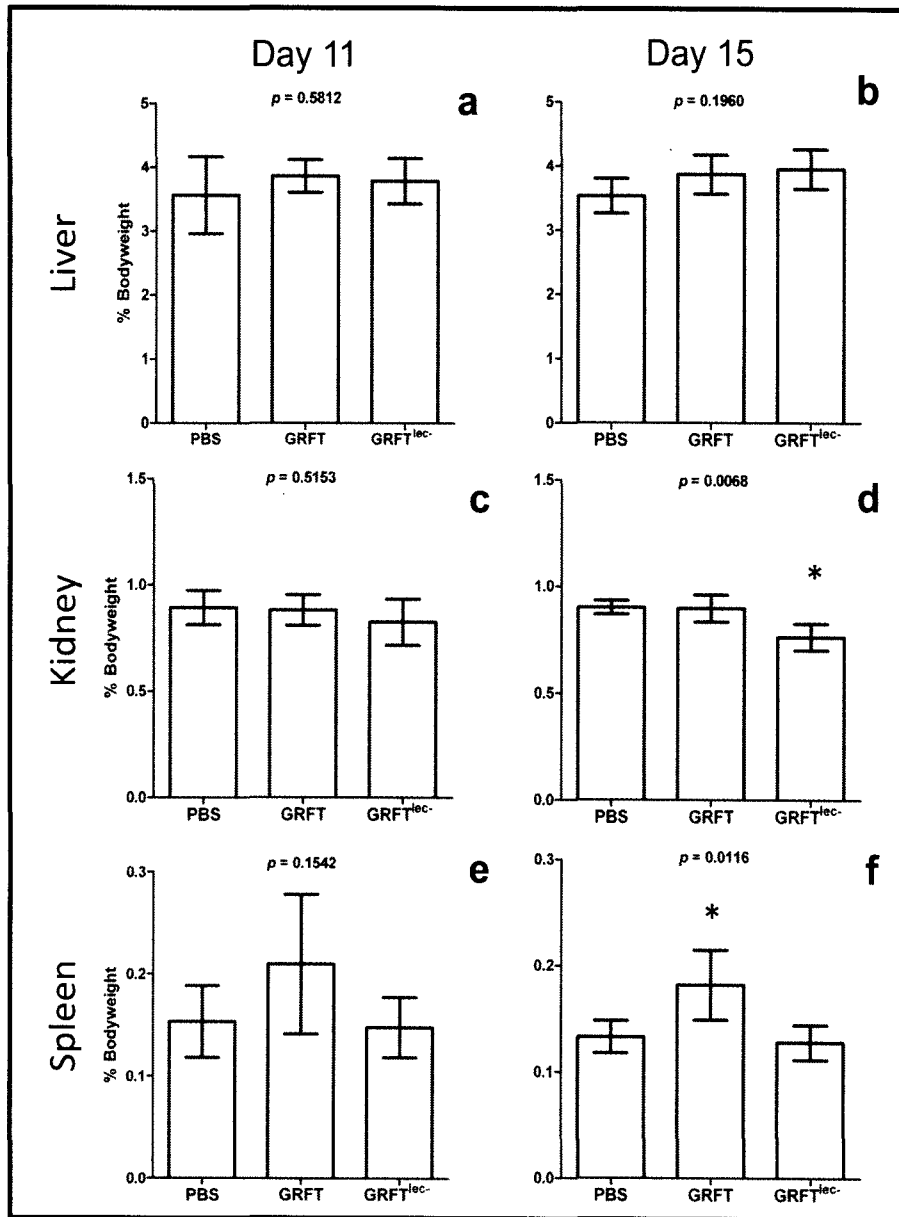


Figure 2.4. Mean organ weight- to-total body weight percentages of treatment groups. Organ weights were determined at sacrifice and normalized by total animal weight. Analysis showed that no statistically significant differences were observed 24 hours post treatments. However, 120 post treatment significant differences in organ weights were observed. Bars indicate standard deviation with significance denoted by (*).

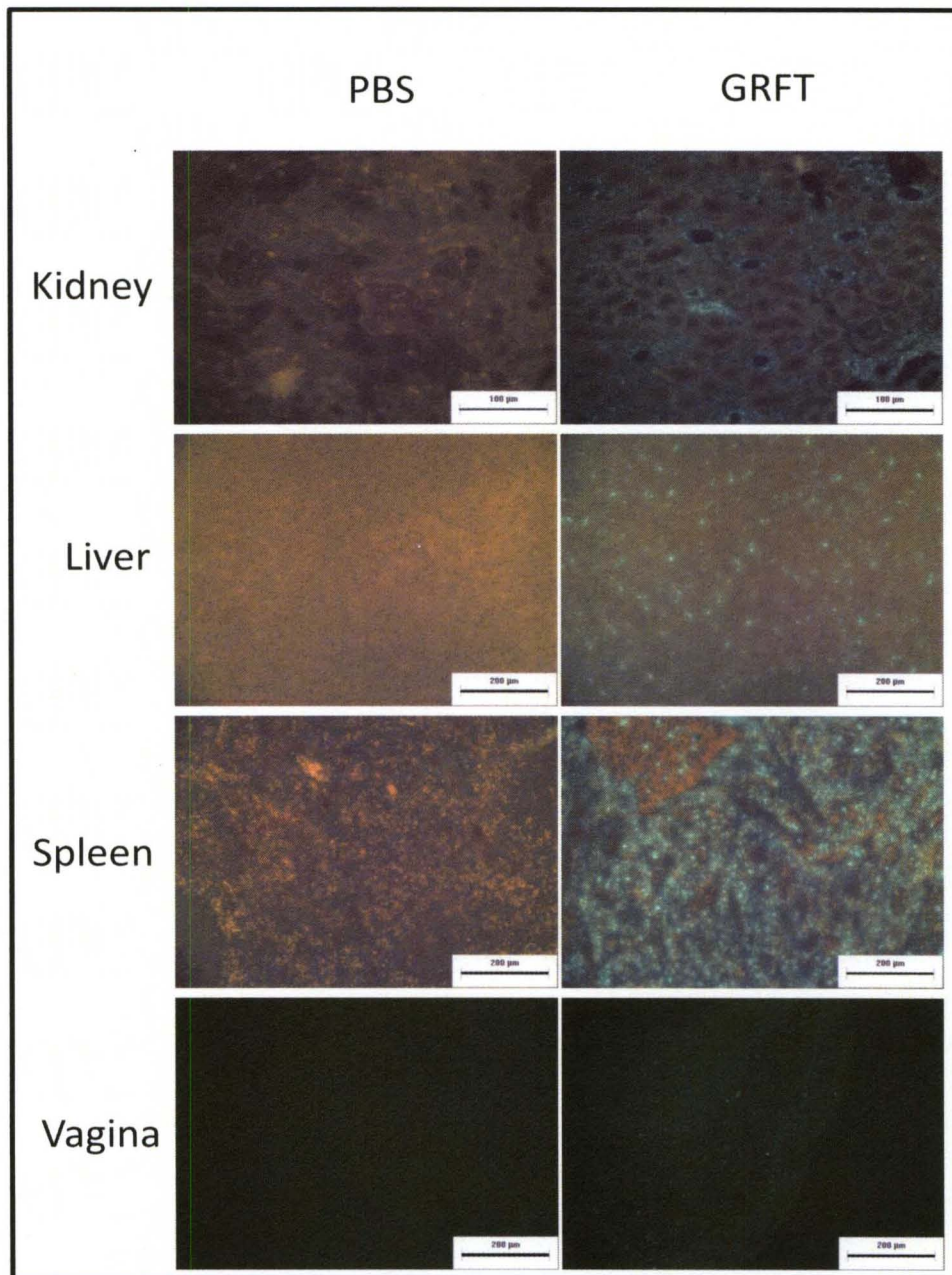


Image 2.2. Immunofluorescent imaging of organ tissues to examine distribution and persistence of GRFT. Unstained organ tissue slides from 120 hours post treatment were probed for GRFT and GRFT^{lec-} presence using rabbit anti-GRFT primary and FITC-conjugated goat anti-rabbit secondary antibodies. GRFT was still observable in kidneys, liver, spleen, and vaginal cross sections. Kidney images at 400x magnification; all others at 200x magnification.

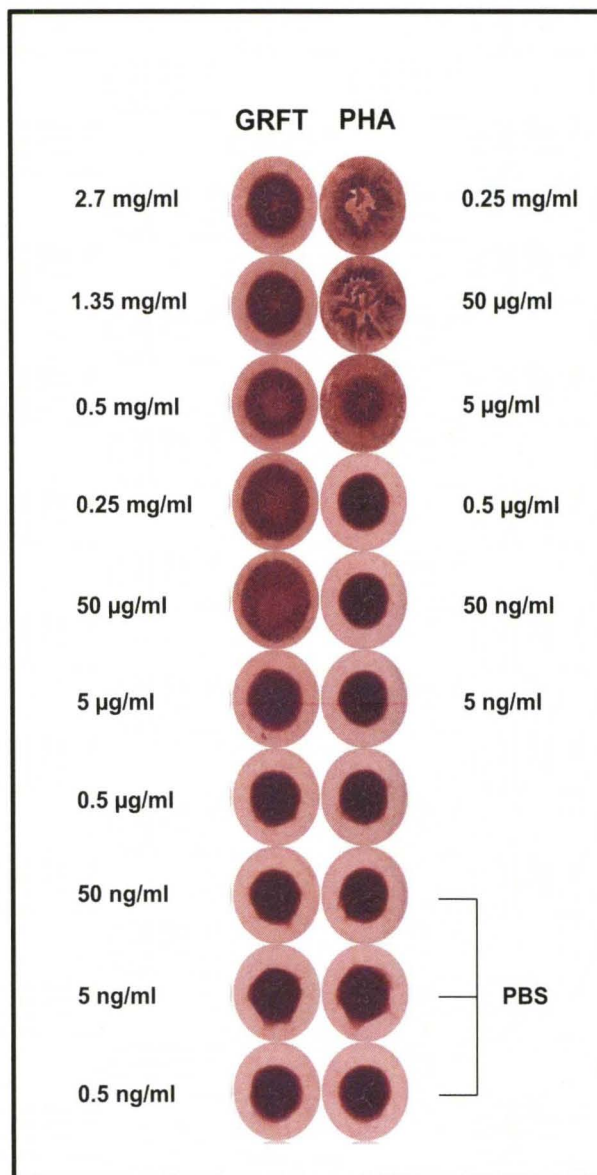


Image 2.3. Hemagglutination activity of GRFT on guinea pig erythrocytes.

Hemagglutination activity of GRFT on guinea pig blood was analyzed.

Phytohemagglutinin (PHA) was used as a positive control. PBS was used as a negative control. Comparison of wells shows that GRFT possesses

hemagglutination activity in guinea pig blood in the range of 1mg/ml (20.5µM) to 100µg/ml (2.05 µM). PHA possesses hemagglutination activity in the 0.5mg/ml (0.15µM) to 10 µg/ml (39 nM) range.

CONCLUSIONS AND FUTURE DIRECTIONS

Griffithsin persists in serum and maintains strong anti-viral activity while simultaneously inducing few systemic changes – an increase in MCV, RDW, and splenomegaly -but displaying no treatment associated organ pathologies. Nonetheless, GRFT does have observable hemagglutination activity in guinea pig blood within the range of treatment doses. This activity may cause the red blood cell variations seen in GRFT treated animals and may account for the splenomegaly observed due to an increase in red blood cell turnover. However, it is currently unclear whether these effects will be observed in other species. Furthermore, in addition to its serum stability and retained anti-viral activity, GRFT shows a wide distribution into organs and vaginal mucosal tissues. These properties support the further examination of GRFT as a potential systemic anti-viral therapy for HIV. Additionally, the translocation into vaginal mucosa may indicate a potential use for GRFT as a pre-exposure prophylactic measure given that GRFT can penetrate into vaginal transudate, which is typically low in protein content.

Previous studies have indicated that while weakly immunogenic, an antibody response to GRFT is possible as a result of chronic dosing. However, it is unclear what impact an antibody response will have upon GRFT's serum persistence, anti-viral activity, and systemic tolerance. We will evaluate the effects of immune activation upon active GRFT serum levels and systemic tolerance utilizing rat and mouse models. We will also generate serum

thermograms of pre-immunized, passively immunized, and chronically exposed animals to assess antibody response impacts on serum protein interactions.

CHAPTER 3

CHARACTERIZATION OF BIOCHEMICAL INTERACTIONS OF GRFT BY EXAMINING ITS IMPACT UPON SERUM PROTEIN PROFILES AND GRFT- PROTEASE INTERACTIONS

INTRODUCTION

In this chapter we examine biochemical interactions that GRFT may have within a living system. We used Differential Scanning Calorimetry (DSC) to evaluate the interactions between GRFT and serum proteins in serum from guinea pigs treated as outlined in Chapter 2. We also characterized human serum spiked with GRFT. Given that GRFT persists in serum and remains active after systemic administration, we tested the drug against a panel of biologically relevant proteases to fully understand GRFT's proteolytic resistance and to characterize potential degradation and metabolic pathways. Finally, we initiated experiments using co-immunoprecipitation of GRFT in serum to identify potential endogenous binding partners.

One method that has been applied to explore biochemical binding interactions in serum or plasma is Differential Scanning Calorimetry (DSC). Plasma consists of over 3000 different proteins but most are present in extremely low abundance with 99% of plasma's proteomic mass consisting of 22 proteins

[94-95]. DSC has been used to measure the denaturation profile, known as a thermogram, of the most abundant proteins present in plasma for healthy individuals as well as those suffering from a number of different diseases [96]. It has been demonstrated that significant differences are apparent between the healthy and disease thermograms presenting the potential for use of this method in the clinical diagnosis of diverse disease states such as rheumatoid arthritis, lupus erythematosus, and Lyme disease [96-100]. The changes in the disease thermogram are proposed to be a manifestation of the interactome hypothesis where low molecular weight proteins or peptides unique to a disease state bind to the more abundant plasma proteins and alter normal interactions between them [101]. DSC is extremely sensitive to changes in concentration of protein components in a mixture as well as to binding interactions between components making this a powerful technique to probe perturbations in the plasma interactome [102]. Measuring a small protein's impact on the more abundant plasma proteins can provide invaluable data to describe stabilizing and destabilizing effects that a protein may have when introduced into a system. Mechanistically, DSC measures small differences in heat flow from a sample and a reference chamber as both chambers are heated at a constant rate over a temperature range of interest [95, 97]. Differences in heat flow as a consequence of thermal events occurring in the sample cell provide a characteristic curve, or thermogram, in the form of excess heat capacity of the sample as a function of temperature [102]. Every protein has a characteristic denaturation thermogram reflecting a unique thermodynamic signature for the melting of the tertiary

structure of that protein [100]. For a mixture of proteins, such as plasma, the thermogram reflects the superposition of the denaturation thermograms of the major protein components according to their relative concentration and the presence of any binding interactions [100]. Observation of changes in the plasma thermogram as a consequence of binding allows the quantification of binding interactions through comparative shifts in denaturation temperatures of the major plasma proteins [102]. For example, a protein ligand which prefers the denatured state of a larger protein will result in a decrease in the denaturation temperature of the larger protein once bound [96]. Thus, it is possible that a consistent and significant change in a serum thermogram may be predictive of toxicity associated with systemic treatment of GRFT by virtue of its impact upon normal interactions between endogenous serum proteins.

In addition to DSC thermograms generated, it was also necessary to investigate GRFT's resistance to proteolysis. In particular, given its presence in vaginal mucosa following systemic administration, GRFT's resistance to a number of proteases in the Kallikrein family was evaluated. The Kallikrein family of proteases are present in blood, vaginal secretions, and semen [103-104]. Furthermore, given GRFT's strong serum persistence, proteases such as Trypsin, MMP-12, and elastase were also evaluated given their strong proteolytic activity and systemic presence.

Finally, we began to examine whether potential endogenous binding partners of GRFT were responsible for its long serum persistence. In particular, hemagglutination assays in species other than guinea pigs were conducted to

expand upon the assays outlined and conducted in Chapter 2. Co-immunoprecipitation of GRFT that had been incubated in serum was used to assess whether there are any endogenous binding partners for GRFT that can be retrieved from serum.

MATERIALS AND METHODS

DSC- Guinea Pig Serum Profiles

Serum samples harvested from guinea pigs injected subcutaneously with PBS, GRFT, or GRFT^{lec-} were aliquotted and subjected to DSC analysis. Samples were dialyzed into 20mM potassium phosphate, 300mM sodium chloride, and 30mM sodium citrate for four days with four buffer changes. Buffer pH was adjusted to 7.5 by the addition of sodium hydroxide solution. Following dialysis, serum samples were diluted in dialysis buffer (1:25) and excess specific heat readings at temperature ranges from 45°C to 90°C were determined using a differential scanning calorimeter (MicroCal VP-Capillary DSC; Instrument software: VPViewer 2000 v.2.0.53). Duplicate runs were completed and average values for each sample were generated. Total protein concentrations were determined via BCA and BGG assays and the concentrations determined were used to normalize DSC readings.

DSC-Human Serum Profiles

For generation of human serum thermogram profiles, dialysis buffer was formulated as before and 3 ml of pooled human serum was dialyzed for a period of four days at 4C. Following dialysis, serum was filtered through a 0.45 micron filter and 99 μ l aliquots were made for spiking with GRFT, GRFT^{lec-}, or PBS. Dialysis buffer, to serve as a reference, was sterile filtered and stored at 4°C. GRFT and GRFT^{lec-} dilutions in PBS were prepared ranging from 20,000 nM to 100 nM. Dialyzed serum aliquots were spiked with GRFT, GRFT^{lec-}, or PBS by the addition of 1 μ l of GRFT dilution to the 99 μ l of dialyzed serum. The resulting

final concentrations ranged from 1nM to 200nM, respectively to cover the ranges of GRFT concentrations observed in guinea pig serum after subcutaneous dosing. Spiked serum samples were diluted in dialysis buffer (1:25) and excess specific heat readings at temperature ranges from 45°C to 90°C were determined using a differential scanning calorimeter. As before, BCA and BGG assays were conducted and total protein concentrations were used to normalize thermogram readings.

Protease Resistance

GRFT's resistance to proteolytic degradation was evaluated using a number of proteases of the Kallikrein family known to be present in blood, seminal fluid and vaginal fluid. Recombinant Kallikrein proteases 3, 5, 7, 11, 12, and 13 (R&D Systems) were reconstituted and activated according to manufacturer recommended activation protocols. In addition to Kallikrein proteases, MMP-12 (R&D Systems), neutrophil elastase (Sigma), and Trypsin (R&D) were also chosen for evaluation. All proteases were reconstituted and activated, if necessary, per manufacturer's instructions.

To approximate both vaginal and seminal fluid environments, vaginal and seminal simulant fluids were formulated according to Owen and Katz [105-106]. In both vaginal and seminal simulant solutions, BSA was omitted in order to avoid potential quenching activity by the BSA. Vaginal simulant solution pH was adjusted by the addition of HCL. Sodium hydroxide solution was used to adjust the pH of the seminal fluid simulant.

In addition to seminal and vaginal fluid simulants, assay buffers were prepared according to the manufacturer's directions to serve as optimal activity conditions for each protease. For neutrophil elastase, a buffer of 50 mM ACES buffer pH 7.2 with 50 μ M Ca/Mg was used for optimal activity conditions

To test GRFT's proteolytic resistance, 2.5 μ l of GRFT (5.4 mg/ml) was combined with 20 μ l of activated protease and 17.5 μ l of either optimal activity buffer, seminal fluid stimulant, or vaginal fluid simulant. After addition of GRFT, samples were vortexed and split evenly between two Eppendorf tubes and incubated for either 1 or 6 hours at 37°C. Ten microliter (10 μ l) aliquots of protease mixture in optimized assay buffer were analyzed by mass spectrometry by direct infusion of the mixture into the instrument. Remaining samples for all proteases were analyzed by either SDS-PAGE or Western blot to assess GRFT degradation. Degradation was considered positive if there were a loss or substantial decrease in intensity of the GRFT 12.5 kD protein band or if deconvoluted mass spectra showed appearance of degradation products.

Hemagglutination

GRFT's hemagglutination activity in other species aside from guinea pig was analyzed. To test GRFT's hemagglutination activity, human, mouse, and sheep erythrocytes (Innovative Research) were washed with PBS to remove cell degradation and lysis products. Cells were spun down at 1000 x g for one minute and resuspended at a final concentration of 2% in PBS containing 3 g/L BSA and 1 g/L sodium azide. Serial dilutions of either Phytohemagglutinin (PHA) (positive control) or GRFT were mixed with an equal volume of erythrocytes in a 96 well

round bottom plate (total 100 μ L/well) and incubated for 1 hr at room temperature, followed by overnight at 4°C. Plates were then allowed to dry. Hemagglutination activity was determined by examination of erythrocyte aggregation or dissemination in comparison to positive and negative control wells. Positive hemagglutination activity was indicated by diffuse blood cells along the bottom of the dried plate, denoting formation of a lattice structure due to agglutination of multiple erythrocytes. Negative hemagglutination activity was observed as a single dot on the bottom of the well, indicating no cell cross-linking.

Co-Immunoprecipitation of GRFT from human serum

Indirect co-immunoprecipitation of GRFT binding ligands in human serum was performed using Dynabeads. Briefly, Dynabeads coated with sheep anti-rabbit IgG were used to precipitate rabbit anti-GRFT antibodies that were either incubated with human serum containing GRFT or pre-coated with GRFT.

4.5 ml human serum (Innovative Research) was aliquotted into 15 ml tubes. 4.5 ml of PBS was added to each flask to dilute serum for easier magnetic separation. Dynabeads at a concentration of 6.7×10^6 beads/ml were separated into four- 500 μ l aliquots. Four test groups were set up for analysis as outlined below.

For test Group A, serum, PBS, and 500 μ l Dynabeads were combined and incubated at 4°C overnight with gentle agitation. For test Group B, 500 μ l Dynabeads was allowed pre-bind to 6 μ g of rabbit anti-GRFT antibodies for one hour at 37°C. After incubation, beads were placed on a magnetic rack for

separation and supernatant containing unbound antibodies was removed and discarded. Beads were then washed twice PBS. After a final magnetic separation, Dynabeads were resuspended in 500 μ l of PBS and added to serum and PBS.

For test Group C, 500 μ l of Dynabeads were combined with 6 μ g of rabbit anti-GRFT antibodies and an excess of GRFT (200 μ g) for one hour at 37°C. As before, after incubation, beads were placed on a magnetic rack for separation and supernatant containing unbound antibodies and GRFT was removed and discarded. Beads were then washed twice PBS. After a final magnetic separation, Dynabeads were resuspended in 500 μ l of PBS and added to serum and PBS.

Finally, for test Group D, 500 μ l Dynabeads, 200 μ g GRFT, and 6 μ g of rabbit anti-GRFT antibodies was added to PBS and serum simultaneously to avoid pre-binding of any of the proteins and antibodies.

All test groups were incubated overnight at 4°C with rotation to facilitate protein binding. After overnight incubation at 4°C, Dynabeads were separated from the samples via magnetic separation. Supernatant was removed via pipette and beads were resuspended in 8 ml PBS for washing. Beads and PBS were mixed for two minutes by gentle rocking of the test tube. After thorough mixing, tubes were placed on a magnetic rack for separation and the supernatant was removed and discarded. The washing process was repeated with an additional 8 ml of PBS and samples were prepared for protein elution.

Elution of the isolated rabbit anti-GRFT antibody, GRFT, and GRFT-protein complexes were performed via pH shift to denature the bead bound antibodies. Briefly, 75 μ l of 0.1M citrate buffer of a pH of 2.7 was added to immobilized beads. Samples were gently mixed via pipetting for two minutes. Following mixing, tubes were placed on a magnetic strip and the supernatant containing Ig, GRFT, and protein complexes was transferred to an Eppendorf tube. The elution process was repeated with an additional 75 μ l of citrate buffer and samples from both elutions were combined. GRFT and protein presence in eluates was examined via SDS-PAGE and Western blot. Eluates were also subjected to mass spectrometry for analysis and identification of any proteins eluted from the co-immunoprecipitation samples.

For identification by mass spectrometry, protein samples were dried by speedvac and dissolved with 8 M urea in 50 mM NH_4HCO_3 (pH 8). Samples were then reduced with dithiothreitol, alkylated with iodoacetamide, diluted with 50 mM NH_4HCO_3 and digested with trypsin at 37°C overnight. Trypsin digests were desalted with C_{18} spin column (Pierce, Rockford, IL) and concentrated by speedvac. Concentrated samples were then loaded on to a C_{18} μ -Precolumn Cartridge from Dionex (Sunnyvale, CA) and peptides in the samples were separated with a packed C_{18} capillary column with an acetonitrile and 0.1% formic acid gradient by a nanoAcquity LC system. The eluted peptides were directed to a LTQ Orbitrap XL mass spectrometer (Thermo Fisher Scientific, San Jose, CA) via a nanospray source and MS/MS spectra of the peptides were acquired by data dependent scan with mass resolution of 100,000 and 7,500 in

MS and MS/MS mode respectively. The database search was performed by Proteome Discoverer 1.2 from Thermo Fisher Scientific with SEQUEST algorithm and SwissProt database (Feb 8, 2011). Only proteins with minimum of 2 distinguish high confident peptide matches (XCorr score 1.9, 2.3 and 2.6 for precursor ion charge state 2, 3, and 4 respectively) were reported as positive identifications.

RESULTS

DSC- Guinea Pig Serum Thermograms

Serum from guinea pigs treated with GRFT and GRFT^{lec-} displayed a substantial shift in excess specific heat capacity versus control animals treated with PBS (Figure 3.1). Group member thermograms were averaged and excess specific heat capacity was plotted against temperature. Groups 2a and 3a (24 hours after last treatment) displayed the greatest increase in excess specific heat capacity, with Groups 2b and 3b (120 hours after last treatment) continuing to display a discernable increase in excess specific heat capacity. GRFT or GRFT^{lec-} treated groups also displayed a nominal increase in the temperature at which the serum thermograms peaked. However, comparisons between time points demonstrated that as GRFT or GRFT^{lec-} concentrations decreased in serum, average serum thermograms began to approach values obtained from PBS treated control groups.

DSC- GRFT and GRFT^{lec-} spiked human serum

Human sera spiked with varying concentrations of GRFT did not display a substantial shift in thermograms versus PBS-spiked control serum. (Figure 3.2). Furthermore, at all concentrations tested, with the exception of 100 nM GRFT, GRFT spiked serum showed a minor decrease in excess specific heat capacity in the first peak of the serum thermogram.

Human sera spiked with varying concentrations of GRFT^{lec-} also did not display a general shift in serum thermograms profiles versus PBS-spiked control serum. (Figure 3.3). However, at 1nM concentrations of GRFT^{lec-}, there appears

to be a greater magnitude of decrease in excess specific heat capacity as compared to other molarities. Nonetheless, visual comparisons between GRFT and GRFT^{lec}-spiked groups did not display any characteristic differences in serum thermogram profiles between the groups.

Protease Resistance

GRFT was resistant to all proteases tested, under all assay conditions, and at all time points tested. Six-hour incubations of GRFT with various kallikrein proteases and MMP-12 in optimized protease activity buffers was visualized using SDS-PAGE analysis with Coomassie blue staining (Image 3.1). Comparisons between the GRFT standard and the GRFT present in protease incubated samples does not reveal any substantial degradation or decrease in intensity of the GRFT band. These results were also observed samples incubated in vaginal and seminal simulant fluids at both 1 hour and 6 hours.

GRFT resistance to all proteases tested was also confirmed via mass spectrometry. Selected deconvoluted spectra from GRFT incubated with proteases are shown in Figure 3.4. A GRFT-only control was used to determine typical fragmentation. Analysis of deconvoluted spectra from samples incubated in optimized protease activity buffers did not reveal substantial GRFT degradation at any time point tested.

Hemagglutination

GRFT's hemagglutination activity in sheep, human, and mouse blood was analyzed (Image 3.2). Visual inspection of wells containing suspended blood samples, PHA, PBS, and GRFT were conducted. As expected, PBS did not

exhibit any hemagglutination activity in any species. PHA, a lectin with known hemagglutination activity, demonstrated activity in the 0.5 mg/ml to 10 µg/ml range (0.3µM to 78.1 nM range). Comparisons between wells demonstrated that GRFT did not possess hemagglutination activity in human, sheep, or mouse samples (mouse samples not shown) at any of the GRFT concentrations tested.

Co-Immunoprecipitation of GRFT from Human Serum

Co-Immunoprecipitation of GRFT/serum complexes was moderately successful. GRFT was captured from serum using the method described above, but at substantially less quantities than expected. Western blot analysis of co-immunoprecipitation eluates demonstrated that groups C and D recovered detectable amounts of GRFT from serum incubations. Mass spectrometric analysis of the eluates revealed a number of proteins were retrieved from the serum by the various groups (Figure 3.5). After eliminating kartinocyte related proteins and proteins retrieved by non-GRFT bound beads, a number of candidate binding partners were identified.

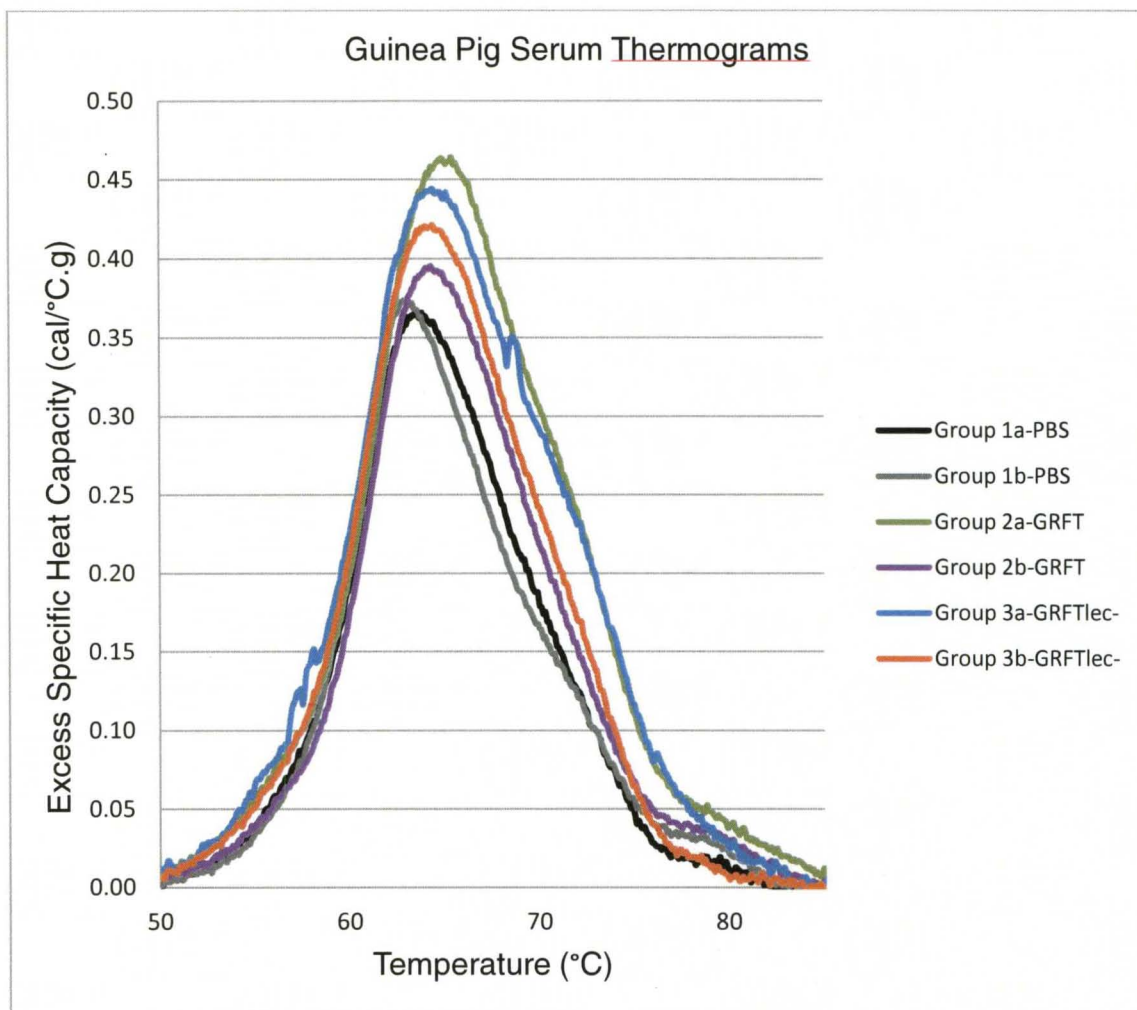


Figure 3.1. Mean serum thermograms of guinea pig groups treated with PBS, GRFT, or GRFT^{lec-}. Excess specific heat capacity of guinea pig serum averaged amongst groups was plotted against temperature to generate serum thermograms. As compared against control groups 1a and 1b, GRFT and GRFT^{lec-} treated animals displayed an overall increase in excess specific heat capacity as well as a small increase in temperature peak. Intra-group comparisons of GRFT and GRFT^{lec-} treatment groups show a decrease in specific heat and temperature at 120 hours post treatments vs. 24 hours post treatments.

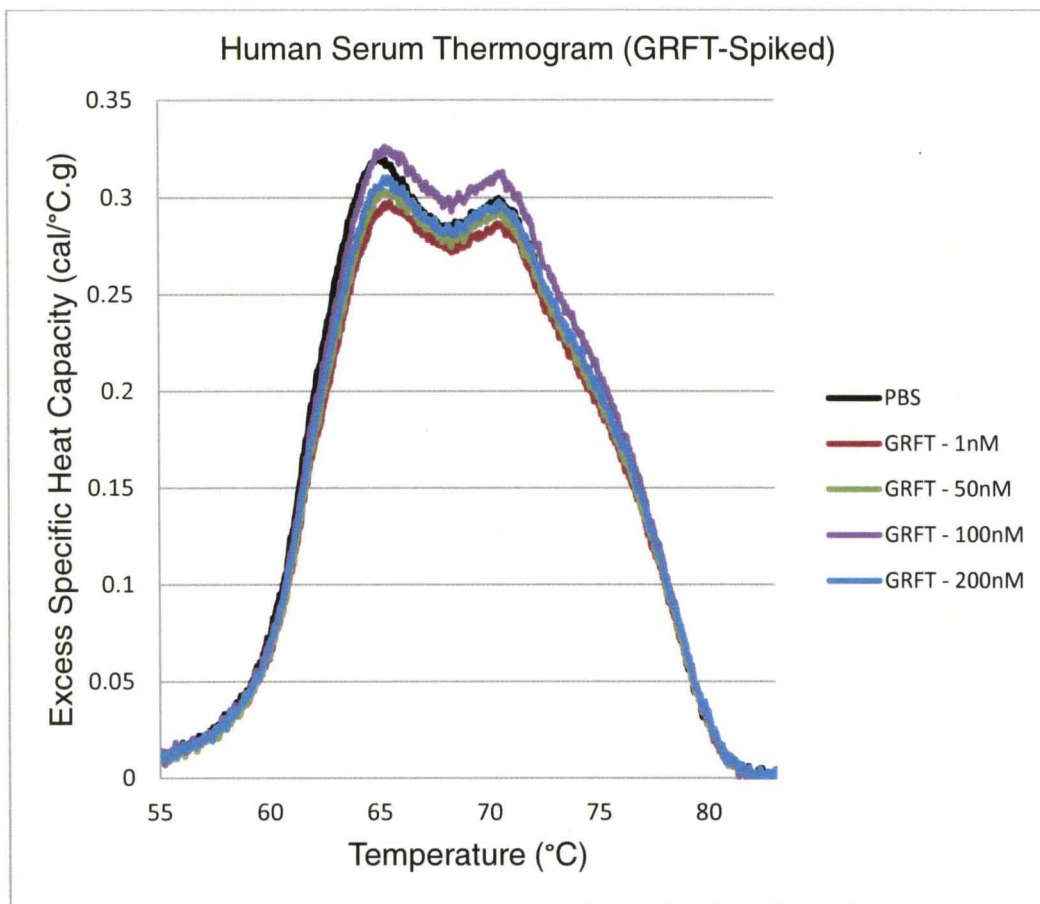


Figure 3.2. Thermogram of human serum spiked with varying concentrations of GRFT. Human serum was spiked with varying concentrations of GRFT and excess specific heat capacity was plotted against temperature to generate thermograms. Spiking of serum with GRFT at the concentrations listed above did not result in substantial changes in serum thermograms. Only one spiking group, 100nM GRFT, showed a nominal increase in excess specific heat capacity versus serum spiked with PBS.

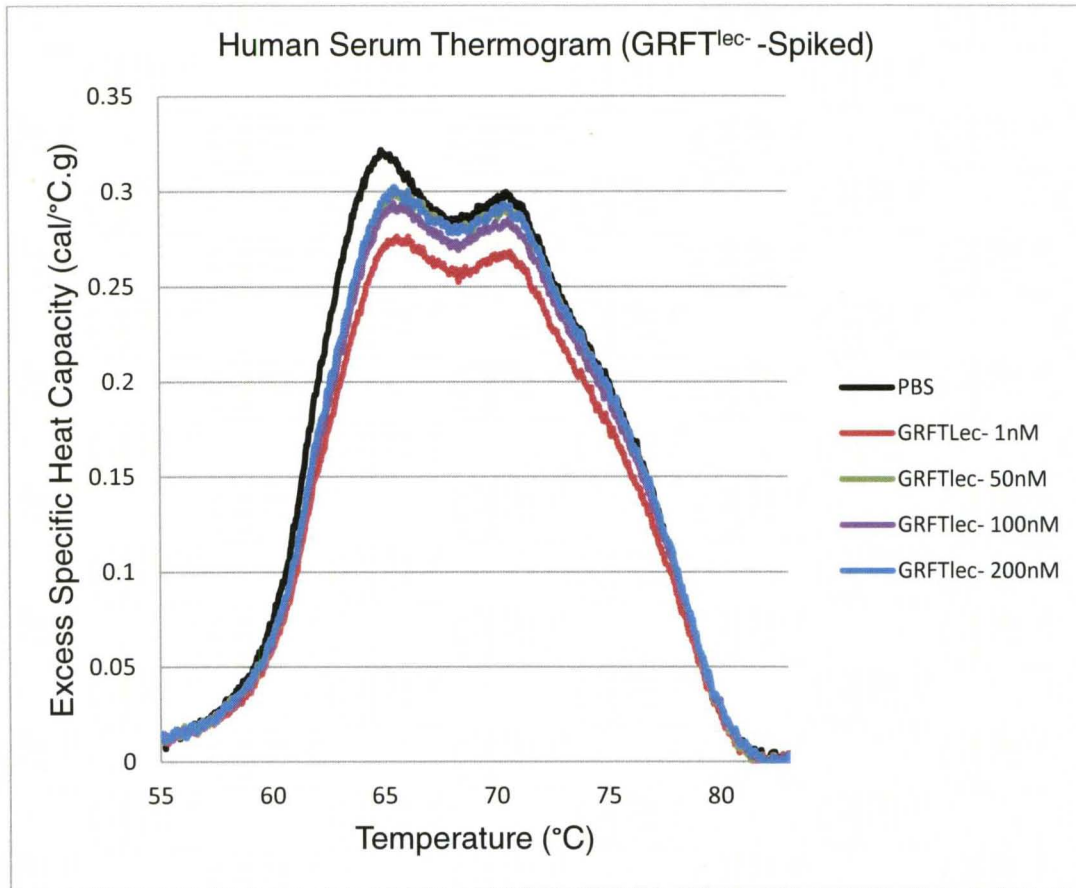


Figure 3.3. Thermogram of human serum spiked with varying concentrations of GRFT^{lec-}. Human serum was spiked with varying concentrations of GRFT^{lec-} and excess specific heat capacity was plotted against temperature to generate thermograms. Spiking of serum with GRFT at the concentrations listed above did not result in an increase in excess specific heat. However, at 1nM concentrations of GRFT^{lec-}, serum samples appeared to have a decrease in excess specific heat capacity.

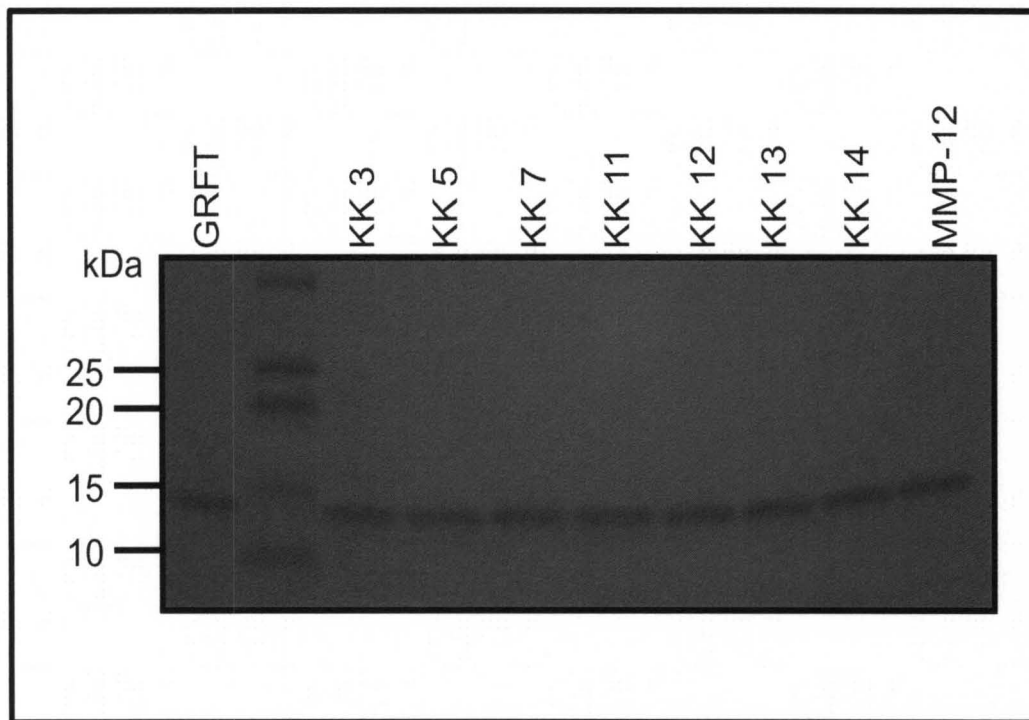


Image 3.1. SDS-PAGE gel of six-hour incubations of GRFT with various proteases. GRFT was exposed to different proteases and incubated for 6 hours in optimized protease activity buffers. GRFT did not display any significant degradation from any of the proteases tested.

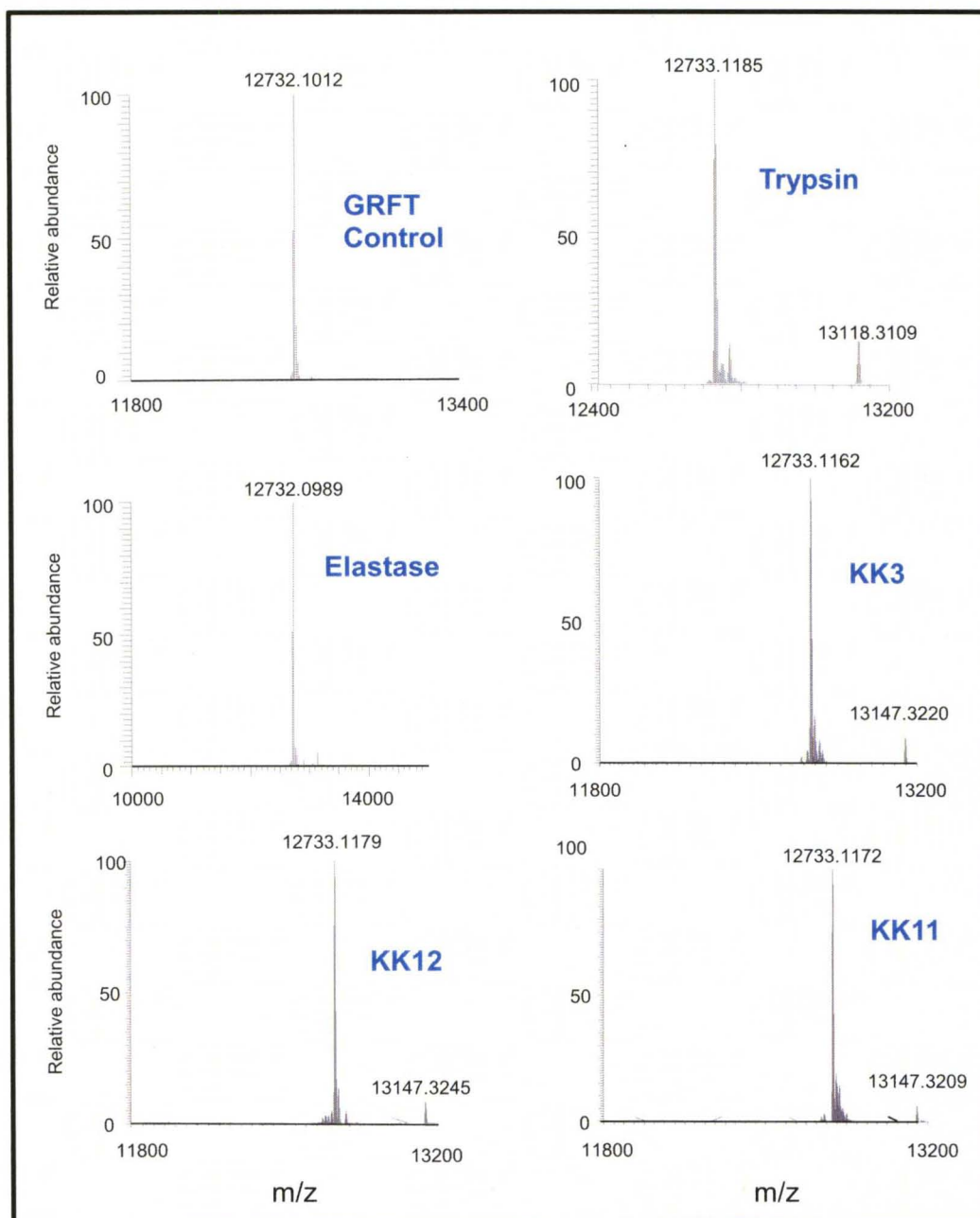


Figure 3.4. Selected mass spectra of GRFT digestions. Six-hour incubations of GRFT with proteases in optimized activity buffers were analyzed by mass spectrometry. Deconvoluted mass spectrometry analysis of directly infused confirmed that GRFT did not experience any significant degradation from the proteases tested.

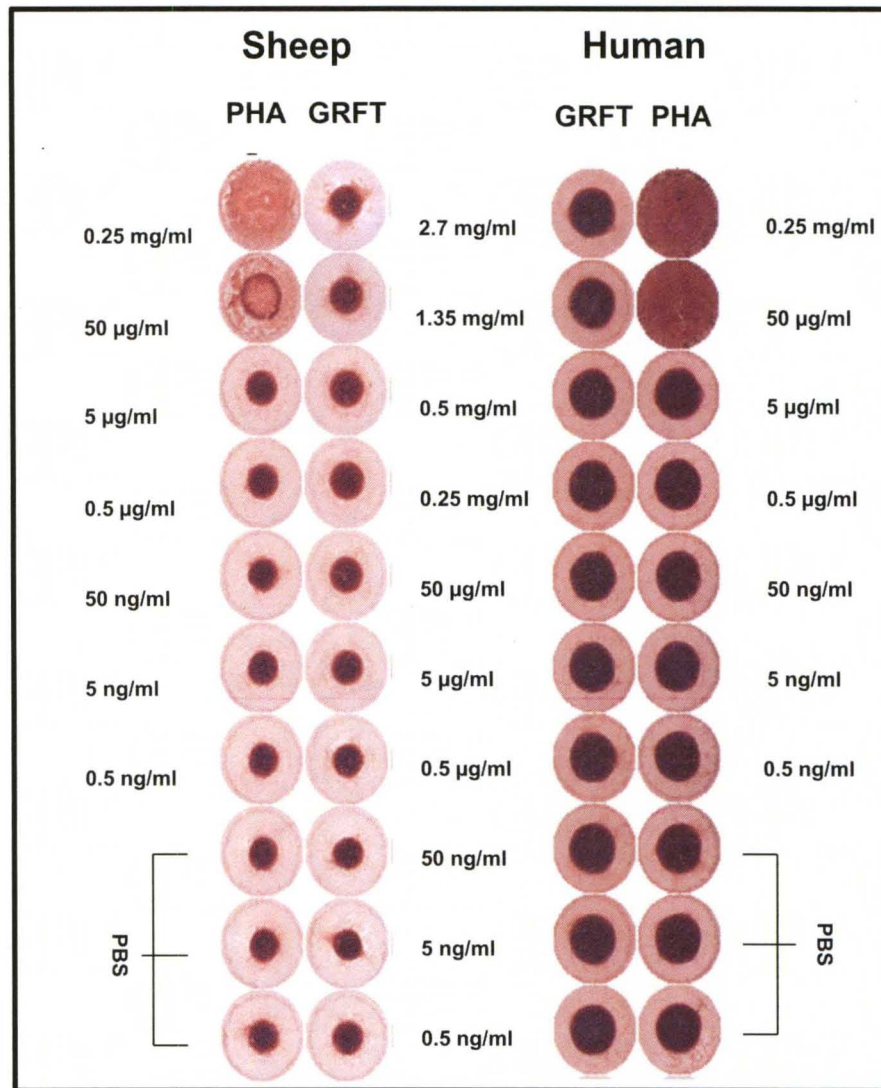


Image 3.2. Hemagglutination activity of GRFT on human and sheep erythrocytes. Hemagglutination activity of GRFT on human and sheep erythrocytes was analyzed. Phytohemagglutinin (PHA) was used as a positive control. PBS was used as a negative control. Comparison of wells shows that GRFT did not display Hemagglutination activity on either sheep or human blood in any of the ranges tested.

Unique Human Co-IP Products	
Group C (GRFT pre-bound to Dynabeads)	Group D (GRFT, not pre-bound to Dynabeads)
14-3-3 protein sigma	Apolipoprotein E
14-3-3 protein zeta/delta	Attractin
Actin, cytoplasmic	Complement C4-A
Apolipoprotein E	Plasminogen
Complement C4-A	
Heat shock 70 kDa protein 1A/1B	
Heat shock protein beta-1	
Putative annexin A2-like protein	
Serotransferrin	

Figure 3.5. Human serum proteins acquired via GRFT co-immunoprecipitation using Dynabeads. Co-immunoprecipitation products for groups A, B, C, and D were analyzed. Control Groups A and B products were non-specific binding products of Dynabeads or polyclonal rabbit anti-GRFT antibodies. The table above represents the final products of Groups C and D, after excluding non-specific protein binding and keratinocyte related proteins.

CONCLUSIONS AND FUTURE DIRECTIONS

DSC

Systemic administration of GRFT may result in changes in serum thermograms that are not observable in GRFT-spiked serum. Given the changes observed in guinea pig serum of treated animals versus controls, GRFT administration may be having some impact on either the serum interactome or inducing changes in major serum protein components. Furthermore, in contrast to serum thermogram changes observed in GRFT and GRFT^{lec-} treated guinea pigs, spiking of human serum with GRFT and GRFT^{lec-} did not result in a substantial shift in serum thermogram profiles. As such, it is currently unknown whether the difference in thermogram shift results is a product of inter-species differences, changes in serum proteins, or changes in protein interactions. Further experiments are required in order to determine GRFT's impacts upon serum thermograms as well as to identify potential endogenous binding partners.

Proteolytic Resistance

GRFT has displayed a strong proteolytic resistance to all proteases tested. Accordingly, GRFT continues to be a strong candidate for systemic administration given that it remains active when exposed to diverse proteases that it may encounter both in vaginal tissues as well as in systemic circulation.

Co-immunoprecipitation

GRFT is immunoprecipitated from human serum by use of anti-GRFT antibodies. Additionally, potential serum binding partners of GRFT were able to be isolated and identified by co-immunoprecipitation and mass spectrometry.

However, refinement of the immunoprecipitation protocols is needed to increase the efficiency of the GRFT-protein complex extractions. First, experiments are needed to determine whether the GRFT precipitated from serum is free GRFT that isn't bound to any serum partner. Further, there also exists the possibility that the serum proteins to which GRFT may bind are of such a low quantity that efficient detection and identification will require large amounts of serum to be precipitated. Accordingly optimization of precipitation protocols will be essential in definitively establishing identities of potential serum binding partners for GRFT.

Additionally, the difference in Co-IP products between GRFT pre-bound and GRFT non pre-bound elutions after elimination of non-specific binding products raises the possibility of steric inaccessibility of GRFT once bound to certain proteins. Given that the GRFT pre-bound to beads yielded a greater number of proteins, it would appear that this method would likely provide the greatest source of binding information. However, we cannot exclude the possibility that binding of GRFT to a protein hides the epitopes recognized by the antibodies. Interestingly, the presence of apolipoprotein E in both samples may provide an indication of why GRFT administration resulted in less weight gain during treatment than PBS treated controls. Given apolipoprotein E's role in lipid catabolism, there may be some unseen disruption in this process. However, we cannot rule out the possibility of some inflammatory reaction to the presence of the protein in systemic circulation as a greater contributing factor to the weight difference observations.

Future Directions

In the future, we shall conduct guinea pig and human serum spiking experiments using a greater range of concentrations of GRFT to determine whether thermogram shifts are a result of endogenous serum protein binding, or a currently unrecognized biological toxicity. Additionally, using Differential Scanning Calorimetry, we shall investigate the thermodynamic impact of systemic GRFT treatment, as well as GRFT and GRFT^{lec-} spiking, upon serum to characterize GRFT's impact upon the serum interactome. Further, using 2D gel electrophoresis and commercially available multiplex immunoassays, we intend to examine changes in serum proteins, cytokines, chemokines and other biomarkers resulting from GRFT treatment in rats and mice to determine whether any observable changes are a result of drug presence or a result of endogenous protein binding.

Additionally, using co-immunoprecipitation of GRFT in Human serum, we shall attempt to catalogue potential endogenous binding partners of GRFT. Using mass spectrometry, we shall identify endogenous binding partners as well as determine the effects that binding may have upon endogenous serum interactions.

CHAPTER 4

ANALYSIS OF GRFT RESISTANT HIV STRAIN AND GENERATION OF HIV-ENV PSEUDOVIRUS TO DETERMINE GRFT NEUTRALIZATION CAPACITY

INTRODUCTION

The ability of antiviral and antimicrobial agents to neutralize HIV has been measured through the use of pseudovirus technology [93, 107-108]. Providing many advantages over handling of live HIV particles, Env pseudovirus technology allows for greater reproducibility and precision, as well as allows for the analysis of relative infectivity of individual envelope isolates.

Briefly, 293FT cells, derived from human embryonic kidneys and transformed with the SV40 T antigen, are used to produce high titer lentiviruses due to their high transfectability. Conventionally, two plasmids are used for transfection and pseudovirus production. The first plasmid possesses genes encoding the viral backbone and Tat-genes, but lacking the env gene of HIV. The second plasmid possesses the desired env genes. Co-transfection of the 293FT cells with both plasmids results in the production of pseudovirions that possess envelopes capable of infecting target cells expressing CD4 and the CXCR4 and CCR5 co-receptors, but unable to replicate.

Once produced, pseudovirus particle titers are determined through the usage of TZM-bl cells. TZM-bl cells are HeLa cells which have been engineered to express CD4 and CCR5 in addition to expressing their already present CXCR4 receptors[109]. As such, they are permissive to infection by a wide variety of HIV strains, including HIV, SIV, and Env-pseudotyped viruses. In addition to presenting necessary receptors for infection, this cell line has also been further engineered to contain Tat-responsive reporter genes for luciferase and B-galactosidase [110].

Upon successful infection of TZM-bl cells by env-pseudotyped particles, the Tat gene contained on the env-minus plasmid is delivered into the TZM-bl cells, inducing an increase in the production of luciferase. Relative infectivity, as well as neutralization capacity of various drugs, can thus be measured as a function of luciferase gene expression in the presence of luciferase substrate. As such, it is a useful mechanism for examining the effectiveness of agents which can prevent viral infection since successful infection by the pseudovirus particle will result in an increase in chemiluminescence.

As such, studies into the ability of GRFT to prevent TZM-bl cell infection with Env-pseudotyped particles can provide an important tool in examining the gp120 spike of HIV, a necessary structure for successful infection. Via site directed mutagenesis, changes to the env encoding genes can be made that alter potential N-linked Glycosylation Sites (NLGS). Given antiviral activity GRFT demonstrates through its binding to the high-mannose glycans attached to these

NLGS, the impact of NLGS changes on GRFT's effectiveness can be evaluated and quantitated.

In this chapter we will examine the glycosylation states of Du156.12, an HIV isolate that is susceptible to neutralization by GRFT, as well as Du156.R18, an HIV isolate which has acquired resistance to GRFT neutralization. Finally, we will describe the production and optimization of HIV env-pseudoviruses that will be used to measure a GRFT neutralization capacity in future experiments wherein antibody responses to GRFT are elicited.

MATERIALS AND METHODS

Gene Sequencing of Du156.12 and Du156.R18

Plasmids of HIV env were supplied by Dr. Montefiori of Duke University. Plasmids containing gp120 and gp41 sequences (cloned into pcDNA3.1) from strains Du156.12 and Du156.R18 (a GRFT-resistant strain of HIV) were provided for analysis and comparison. Competent dh5-alpha bacteria were transformed with the appropriate plasmid containing either Du156.12 or Du156.R18 sequence strands. After transformation, transformed bacterial colonies were isolated by streaking on a plate containing ampicillin for selection. After 12 hours of growth, four (4) colonies from each strain were selected and grown in LB broth overnight at 37C with vigorous shaking. Du156.12 and Du156.R18 env plasmids were then extracted from bacterial cultures via Miniprep (Quiagen) kit per the manufacturer's instructions.

Aliquots of plasmid preparations containing forward and reverse primers for gp120 and gp41 were sent for sequencing. Eleven (11) primers were used for sequence generation (Table 4.1). Sequencing results were aligned and consensus sequences were generated on Sequencher 4.8 software.

Pseudovirus generation

Pseudovirus particles for HIV-env neutralization assays were generated using modified methods previously described [93]. Briefly, 293 FT cells were cultured for transfection with HIV-env containing plasmids. Eighteen (18) hours before transfection, cells were plated at a density of 6×10^6 . On the day of transfection, cells were visually inspected and were 50% confluent. Transfection

media was prepared by combining 120 μ l of Fugene HD, 12 μ g of endotoxin free Du156.12 plasmid, and 48 μ g of pSG3 plasmid in 480 μ l of DMEM. After mixing, the media was allowed to react at room temperature for 30 minutes. At the end of 30 minutes, the reaction mixture was added in a drop-wise manner to plated 293FT cells with gentle swirling of the cell culture plate.

Plates of transfected cells were allowed to incubate at 37°C for a period of 5 hours. At the end of 5 hours, transfection media was removed and replaced with fresh media. Transfected cells were placed in a 32°C incubator with 5% CO₂ and allowed to incubate for a period of 72 hours. At the end of 72 hours, media containing pseudovirus particles was collected, centrifuged at 1000 x g for 15 minutes, and aliquotted for pseudovirus titration.

Pseudovirus Titration

Titration of media containing pseudovirus particles was conducted via titration in TZM-bl cells to probe for changes luciferase expression due to successful infection with pseudovirus particles containing the luciferase promoter gene. Briefly, serial dilutions of pseudovirus stock ranging from undiluted to a dilution of 1:78125 were placed into 96-well white tissue culture plates, by addition of pseudovirus stocks to wells containing 100 μ l of media (DMEM with 10% FBS - no phenol red) in all wells. 100 μ L of TZM-bl cells at a density of 100,000 cells/ml in media (DMEM with 10% FBS- no phenol red) were added to all wells and incubated at 37°C for 72 hours. Cells only wells, containing no pseudovirus stock were used as background-luciferase production controls. At the end of 72 hours, culture media was removed and the cells were gently

washed by the addition of 200 μ l of PBS. PBS was removed and cells were lysed by addition of 50 μ l of room temperature lysis buffer and 30 minutes of vigorous shaking. Luciferase detection reagent was prepared by dissolving the luciferase assay substrate in 10 mL of luciferase assay buffer. After cells were lysed, luciferase activity was measured by the addition of 100 μ l of luciferase detection reagent to each sample well. Chemiluminescence was read immediately.

RESULTS

Gene Sequencing of Du156.12 and Du156.R18

Sequencing of Du156.12 and Du156.r18 revealed a number of glycosylation changes in the Du156.r18 gp120 sequence that resulted in four glycosylation site deletions and one glycosylation site addition (Figure 4.1). Two glycosylation site deletions, one at the beginning of the V3 domain and one between the V4 and V5 domains were the result of base changes which resulted in the Asn-X-Ser/Thr sequon being eliminated. Namely, the sequon deletion at the beginning of the V3 domain of Du156.R18 was the result of an Asparagine being substituted with a Serine residue. The sequon deleted between V4 and V5 was the result of a Threonine being substituted with an Isoleucine residue in the N-X-T sequon.

However, residue substitution was not the only mechanism by which Du156.R18 modified its NLGS. Two of the four potential N-linked glycosylation site deletions were the result of a 30 amino acid deletion in the V1/V2 loop, which resulted in a shortening of the V1/V2 loop by 10 residues. In contrast to the glycosylation site deletions, there was the addition of one glycosylation site at residues 341-343 by the substitution of Threonine for Alanine, which resulted in the creation of a N-linked glycosylation site sequon.

Pseudovirus Generation and Titration

Titration of Pseudovirus particle containing media in TZM-bl cells revealed a successful creation of infective Du156.12 pseudoparticles (Figure 4.2). Chemiluminescence, expressed in Relative Luminescence Units (RLU) was

plotted against virus stock dilution. Titre results showed that undiluted virus stocks resulted in an almost 6 fold increase in luciferase expression in TZM-bl cells, producing an average RLU of 20448. Furthermore, this increased expression was observable at even the lowest viral concentrations tested (1:78125 dilution of virus stocks). Background TZM-bl luciferase activity was determined to be 3600.

Sequence Name	Sequence 5' to 3'
GRFTr1	ATGTGTAAGGTGGCGGG
GRFTr2	CACAAGCCTGTCCAAAGG
GRFTr3	TTGAACCACCCTCAGGAG
GRFTr4	TGCTGCTCCCAAGAACC
GRFTr5	GGGTCTGAAACGACAAAGG
Gp120f	TAATGTGTAAGGTGGCGGG
chimerolap1	AGGCTTGTGTTATGGTTGAGG
chimeraolap2	CATAACACAAGCCTGTCCAA
gp120r	ACAGCTCCTAGTCCCCTG
Du156f	CGAAGCACTCCTCCAAGTAA
Du156r	GGGTCTGAAACGACAAAGG

Table 4.1. Primers used for Du156 sequencing. The above forward and reverse primers were used to generate consensus sequences of plasmids containing HIV-env Du156.12 and Du156.R18.

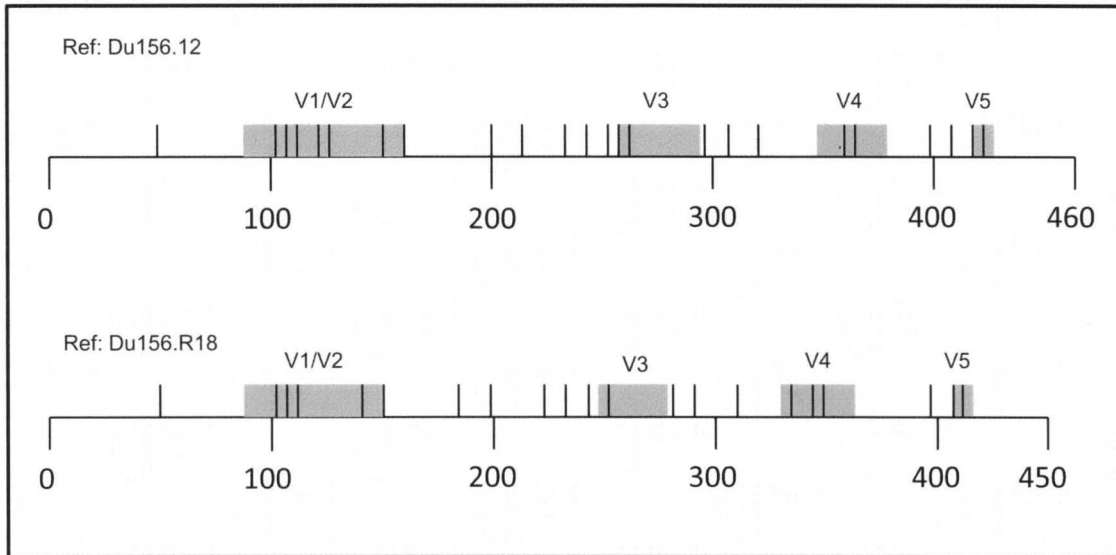


Figure 4.1. Potential N-linked glycosylation sites (NLGS) of gp120 of Du156.12 and Du156.R18. Sequencing analysis of Du156.12 and Du156.R18 revealed a number of NLGS changes. Sequons of Asn-X-Ser and Asn-X-Thr, where X ≠Pro were recorded. Two (2) NLGS were deleted by removal of 10 amino acid residues (SSATYNNSMN) in the V1/V2 loop of Du156.R18. Du156.R18 also displayed a deletion of one NLGS in V3, an addition of one NLGS in V4, and a deletion of one PNGS near residue 400. Total NLGS for Du156.12 totaled 24, whereas Du156.R18 had a total of 21 NLGS.

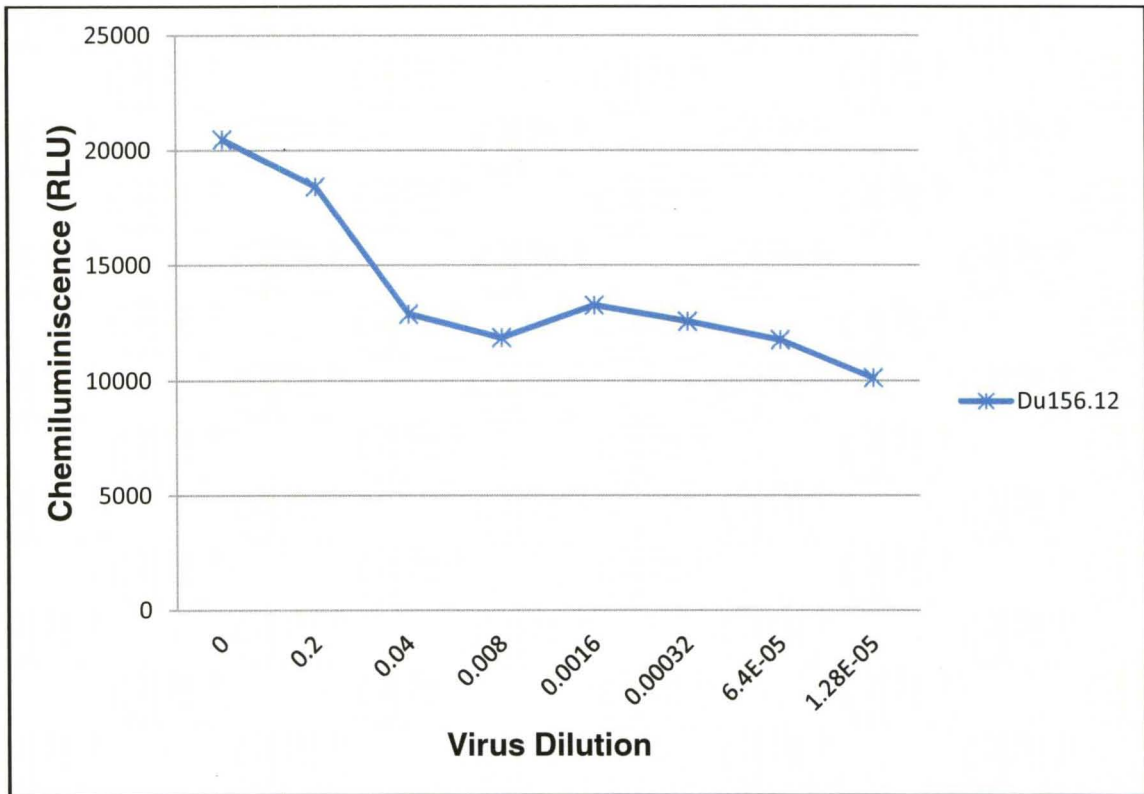


Figure 4.2. Pseudovirus titre of Du.156.12 in TZM-bl cells. Analysis of pseudovirus production in 293FT cells for GRFT neutralization assays demonstrated production of infective HIV-env virions. Undiluted samples displayed an average chemiluminescence reading of 20448 Relative Luminescence Units (RLU). At a 1:78125 dilution of pseudovirus stocks, chemiluminescence was still detectable, with an average rating of 11748 RLU. Cells-only background wells displayed an average RLU of 3600.

CONCLUSIONS AND FUTURE DIRECTIONS

Gene Sequencing of Du156.12 and Du156.R18

Differences in NLGS between DU156.12 and Du156.R18 may be responsible for its resistance to GRFT neutralization. With less potential high-mannose glycans present on gp120, GRFT's ability to impede infection of cells may be reduced. However, it is important to note that two of the glycan deletions were a result of a 10 residue deletion in the V1/V2 region of gp120, thus shortening the V1/V2 loop while simultaneously eliminated two NLGS. Previous studies have shown that a shortened V1/V2 loop may result in increased infectivity of viral isolates [56-57]. Accordingly, there may be some synergistic effect between the loss of NLGS and shortening of the V1/V2 loops which promotes viral evasion of GRFT binding while simultaneously allowing closer interaction with cellular receptors necessary for viral infection.

Pseudovirus Generation and Titration

Pseudovirus particles from the Du156.12 strain of HIV will be a useful control for examining GRFT's potential neutralization capacity in other experiments, including long term animal dosing. Accordingly, Du156.12 *env*-pseudoviruses will be a useful starting point for the induction of NLGS changes to observe how GRFT's activity is impacted as NLGS are modified. However, further optimization of the pseudovirus production protocol is needed in order to increase RLUs even higher above background to increase overall assay sensitivity.

Once optimized, the use of this HIV-1 pseudovirus technology will enable us to fully evaluate the impact that an antibody response will have upon the neutralization capacity of GRFT. If continued activity of GRFT is seen in pseudovirus assays despite an antibody response, this finding would indicate that GRFT treatment may be continued even though an antibody response is mounted. However, should GRFT become less active after an immune response is generated, it may indicate that GRFT's usefulness would be limited to short term courses of therapy.

In the future, it would be prudent to determine binding interactions between GRFT and modified gp120 glycans. As mentioned before, pseudovirus neutralization assays are powerful tools to assess GRFT's neutralization capacity versus gp120's possessing modified glycans. Via site-directed mutagenesis, potential NLGS's could be eliminated and HIV-env mutations should be tested against GRFT concentrations in pseudovirus neutralization assays. Additionally, purified gp120-GRFT interactions should be probed using isothermal titration calorimetry, analytical ultracentrifugation, and protein binding assays to explore affinity and avidity interactions between modified gp120s and GRFT in order to evaluate the impact that viral NLGS mutation has upon GRFT's inhibitory capacity.

CHAPTER 5

OVERALL RESEARCH IMPLICATIONS AND APPLICATIONS

HIV treatment

The totality of the research presented in this thesis supports GRFT's utility as a new adjunct therapy to assist in combating chronic HIV infection. As we have demonstrated, GRFT can be maintained in serum at levels far exceeding its anti-HIV-1 EC_{50} . We also showed that GRFT is well tolerated in animals when dosed subcutaneously, with little impact upon organ systems, CBC counts, and serum chemistries. While hemagglutination assays did demonstrate agglutination activity on guinea pig erythrocytes, no such activity was seen in human erythrocytes. Thus it is questionable whether some of the systemic effects observed in guinea pigs would occur in humans.

Given the various mechanisms of the various HAART treatment regimens, GRFT treatment could provide an additional method of interrupting the infection cycle of HIV as well as extending the useful life of current therapies. By preventing fusion with cells, GRFT may be useful in reducing infection of uninfected cells as well as prolonging the usefulness of other anti-HIV therapies by binding to drug resistant escape mutants when viral loads are pushed to undetectable levels. This may effectively decrease the speed with which HIV

acquires resistance to other HAART drugs by denying drug-resistant escape mutants an opportunity to establish a foothold in uninfected cells.

Further research into the systemic effects in other species will be necessary in order to determine whether the tolerability profile observed in guinea pigs is consistent among species. Additionally, research into how an antibody response will impact GRFT's systemic profile and activity are necessary. As a foreign protein capable of generating an immune response, GRFT will have to maintain activity in the face of an immune response given that immunosuppressive options used to reduce the body's response to a proteinacious therapy may not be viable given the nature of HIV infection.

Prophylaxis

GRFT translocation into the vaginal mucosa also supports GRFT's utility in combating HIV, albeit in a different manner. With GRFT being found present in vaginal mucosal washes, systemic GRFT treatment provides the opportunity to have GRFT persistently at one of the major portals of infection- the vaginal mucosa. Accordingly, GRFT may prove to be a second line protection useful for serodiscordant partners should longer term GRFT immunotherapy become a viable pre-exposure prophylaxis modality.

Immunotherapy

As has been demonstrated before, HIV-1 resistance to GRFT and other lectins has entailed the removal of high mannose glycans via alterations in N-linked glycosylation sites [4, 7, 111]. Burst therapy, the use of the drug over short periods of time, may be a way to encourage viral evolution towards the

removal of epitope obscuring high-mannose glycans. Accordingly, the favorable short term profile that was observed in guinea pigs suggests that should even long term treatment with GRFT not be feasible due to potential immune reactions or unseen toxicities, GRFT may still be a viable tool in combating HIV.

Differential Scanning calorimetry.

Current assays have not demonstrated any toxicities of GRFT. Accordingly, novel methods to identify potential toxicities are necessary fully understand the impact of adding GRFT into a living system. DSC thermograms can be used to measure complex biochemical binding interactions as well as provide potential information into biocomparability. The use of DSC to evaluate the impact of GRFT therapy may ultimately provide a screening mechanism by which to measure potential biological impacts not observable by other methods.

REFERENCES

1. www.UNAIDS.com, retrieved 2/15/2011.
2. Operskalski, E.A. and A. Kovacs, *HIV/HCV Co-infection: Pathogenesis, Clinical Complications, Treatment, and New Therapeutic Technologies*. Curr HIV/AIDS Rep, 2011. **8**(1): p. 12-22.
3. Bertaux, C., et al., *Entry of hepatitis C virus and human immunodeficiency virus is selectively inhibited by carbohydrate-binding agents but not by polyanions*. Virology, 2007. **366**(1): p. 40-50.
4. Alexandre, K.B., et al., *Mannose-rich glycosylation patterns on HIV-1 subtype C gp120 and sensitivity to the lectins, Griffithsin, Cyanovirin-N and Scytovirin*. Virology, 2010. **402**(1): p. 187-96.
5. Helle, F., et al., *Role of N-linked glycans in the functions of hepatitis C virus envelope proteins incorporated into infectious virions*. J Virol, 2010. **84**(22): p. 11905-15.
6. Balzarini, J., *Targeting the glycans of glycoproteins: a novel paradigm for antiviral therapy*. Nat Rev Microbiol, 2007. **5**(8): p. 583-97.
7. Balzarini, J., *Inhibition of HIV entry by carbohydrate-binding proteins*. Antiviral Res, 2006. **71**(2-3): p. 237-47.
8. O'Keefe, B.R., et al., *Broad-spectrum in vitro activity and in vivo efficacy of the antiviral protein griffithsin against emerging viruses of the family Coronaviridae*. J Virol, 2010. **84**(5): p. 2511-21.
9. Francois, K.O. and J. Balzarini, *Potential of carbohydrate-binding agents as therapeutics against enveloped viruses*. Med Res Rev, 2010.
10. Witvrouw, M., et al., *Resistance of human immunodeficiency virus type 1 to the high-mannose binding agents cyanovirin N and concanavalin A*. J Virol, 2005. **79**(12): p. 7777-84.
11. Zappe, H., M.E. Snell, and M.J. Bossard, *PEGylation of cyanovirin-N, an entry inhibitor of HIV*. Adv Drug Deliv Rev, 2008. **60**(1): p. 79-87.
12. Tanaka, H., et al., *Mechanism by which the lectin actinohivin blocks HIV infection of target cells*. Proc Natl Acad Sci U S A, 2009. **106**(37): p. 15633-8.
13. Emau, P., et al., *Griffithsin, a potent HIV entry inhibitor, is an excellent candidate for anti-HIV microbicide*. J Med Primatol, 2007. **36**(4-5): p. 244-53.

14. Mori, T., et al., *Isolation and characterization of griffithsin, a novel HIV-inactivating protein, from the red alga Griffithsia sp.* J Biol Chem, 2005. **280**(10): p. 9345-53.
15. Varki, A., et. al., Essentials of Glycobiology, 2nd Ed., Cold Spring Harbor, NY., Cold Spring Harbor Press, 2009.
16. Bosques, C.J., et al., *Effects of glycosylation on peptide conformation: a synergistic experimental and computational study.* J Am Chem Soc, 2004. **126**(27): p. 8421-5.
17. Vigerust, D.J. and V.L. Shepherd, *Virus glycosylation: role in virulence and immune interactions.* Trends Microbiol, 2007. **15**(5): p. 211-8.
18. Voet, D., et al., Fundamentals of Biochemistry, 3rd Ed., Hoboken, NJ: Wiley Press, 2008.
19. Alberts, B., et. al., Molecular Biology of the Cell, 5th Ed., New York, NY, Garland Science, 2008.
20. Doores, K.J., et al., *Envelope glycans of immunodeficiency virions are almost entirely oligomannose antigens.* Proc Natl Acad Sci U S A, 2010. **107**(31): p. 13800-5.
21. Douek, D.C., M. Roederer, and R.A. Koup, *Emerging concepts in the immunopathogenesis of AIDS.* Annu Rev Med, 2009. **60**: p. 471-84.
22. Swanson, C.M. and M.H. Malim, *SnapShot: HIV-1 proteins.* Cell, 2008. **133**(4): p. 742, 742 e1.
23. Chan, D.C., et al., *Core structure of gp41 from the HIV envelope glycoprotein.* Cell, 1997. **89**(2): p. 263-73.
24. McDougal, J.S., D.R. Klatzmann, and P.J. Maddon, *CD4-gp120 interactions.* Curr Opin Immunol, 1991. **3**(4): p. 552-8.
25. Choe, H., et al., *The beta-chemokine receptors CCR3 and CCR5 facilitate infection by primary HIV-1 isolates.* Cell, 1996. **85**(7): p. 1135-48.
26. Bjorndal, A., et al., *Coreceptor usage of primary human immunodeficiency virus type 1 isolates varies according to biological phenotype.* J Virol, 1997. **71**(10): p. 7478-87.
27. Berger, E.A., P.M. Murphy, and J.M. Farber, *Chemokine receptors as HIV-1 coreceptors: roles in viral entry, tropism, and disease.* Annu Rev Immunol, 1999. **17**: p. 657-700.
28. Dalglish, A.G., et al., *The CD4 (T4) antigen is an essential component of the receptor for the AIDS retrovirus.* Nature, 1984. **312**(5996): p. 763-7.
29. Sattentau, Q.J. and R.A. Weiss, *The CD4 antigen: physiological ligand and HIV receptor.* Cell, 1988. **52**(5): p. 631-3.
30. Myszka, D.G., et al., *Energetics of the HIV gp120-CD4 binding reaction.* Proc Natl Acad Sci U S A, 2000. **97**(16): p. 9026-31.
31. Cormier, E.G. and T. Dragic, *The crown and stem of the V3 loop play distinct roles in human immunodeficiency virus type 1 envelope glycoprotein interactions with the CCR5 coreceptor.* J Virol, 2002. **76**(17): p. 8953-7.

32. Suphaphiphat, P., M. Essex, and T.H. Lee, *Mutations in the V3 stem versus the V3 crown and C4 region have different effects on the binding and fusion steps of human immunodeficiency virus type 1 gp120 interaction with the CCR5 coreceptor*. *Virology*, 2007. **360**(1): p. 182-90.
33. Briz, V., E. Poveda, and V. Soriano, *HIV entry inhibitors: mechanisms of action and resistance pathways*. *J Antimicrob Chemother*, 2006. **57**(4): p. 619-27.
34. Weiss, C.D., *HIV-1 gp41: mediator of fusion and target for inhibition*. *AIDS Rev*, 2003. **5**(4): p. 214-21.
35. Poveda, E., V. Briz, and V. Soriano, *Enfuvirtide, the first fusion inhibitor to treat HIV infection*. *AIDS Rev*, 2005. **7**(3): p. 139-47.
36. Nawaz, F., et al., *The genotype of early-transmitting HIV gp120s promotes alphabeta-reactivity, revealing alphabetaCD4+ T cells as key targets in mucosal transmission*. *PLoS Pathog*, 2011. **7**(2): p. e1001301.
37. Li, Q., et al., *Peak SIV replication in resting memory CD4+ T cells depletes gut lamina propria CD4+ T cells*. *Nature*, 2005. **434**(7037): p. 1148-52.
38. Zhang, Z.Q., et al., *Roles of substrate availability and infection of resting and activated CD4+ T cells in transmission and acute simian immunodeficiency virus infection*. *Proc Natl Acad Sci U S A*, 2004. **101**(15): p. 5640-5.
39. Zhang, Z., et al., *Sexual transmission and propagation of SIV and HIV in resting and activated CD4+ T cells*. *Science*, 1999. **286**(5443): p. 1353-7.
40. Haase, A.T., *Perils at mucosal front lines for HIV and SIV and their hosts*. *Nat Rev Immunol*, 2005. **5**(10): p. 783-92.
41. Shacklett, B.L., et al., *Mucosal T-cell responses to HIV: responding at the front lines*. *J Intern Med*, 2009. **265**(1): p. 58-66.
42. O'Connor, D.M., *A tissue basis for colposcopic findings*. *Obstet Gynecol Clin North Am*, 2008. **35**(4): p. 565-82; viii.
43. Pudney, J., A.J. Quayle, and D.J. Anderson, *Immunological microenvironments in the human vagina and cervix: mediators of cellular immunity are concentrated in the cervical transformation zone*. *Biol Reprod*, 2005. **73**(6): p. 1253-63.
44. Miller, C.J. and R.J. Shattock, *Target cells in vaginal HIV transmission*. *Microbes Infect*, 2003. **5**(1): p. 59-67.
45. Grivel, J.C., R.J. Shattock, and L.B. Margolis, *Selective transmission of R5 HIV-1 variants: where is the gatekeeper?* *J Transl Med*, 2011. **9 Suppl 1**: p. S6.
46. Chenine, A.L., et al., *Relative transmissibility of an R5 clade C simian-human immunodeficiency virus across different mucosae in macaques parallels the relative risks of sexual HIV-1 transmission in humans via different routes*. *J Infect Dis*, 2010. **201**(8): p. 1155-63.
47. Olsson, J., et al., *Human immunodeficiency virus type 1 infection is associated with significant mucosal inflammation characterized by increased expression of CCR5, CXCR4, and beta-chemokines*. *J Infect Dis*, 2000. **182**(6): p. 1625-35.

48. Nazli, A., et al., *Exposure to HIV-1 directly impairs mucosal epithelial barrier integrity allowing microbial translocation*. PLoS Pathog, 2010. **6**(4): p. e1000852.
49. Poles, M.A., et al., *A preponderance of CCR5(+) CXCR4(+) mononuclear cells enhances gastrointestinal mucosal susceptibility to human immunodeficiency virus type 1 infection*. J Virol, 2001. **75**(18): p. 8390-9.
50. Bomsel, M., *Transcytosis of infectious human immunodeficiency virus across a tight human epithelial cell line barrier*. Nat Med, 1997. **3**(1): p. 42-7.
51. Shen, R., et al., *Dendritic cells transmit HIV-1 through human small intestinal mucosa*. J Leukoc Biol, 2010. **87**(4): p. 663-70.
52. McCoombe, S.G. and R.V. Short, *Potential HIV-1 target cells in the human penis*. AIDS, 2006. **20**(11): p. 1491-5.
53. Patterson, B.K., et al., *Susceptibility to human immunodeficiency virus-1 infection of human foreskin and cervical tissue grown in explant culture*. Am J Pathol, 2002. **161**(3): p. 867-73.
54. Leonard, C.K., et al., *Assignment of intrachain disulfide bonds and characterization of potential glycosylation sites of the type 1 recombinant human immunodeficiency virus envelope glycoprotein (gp120) expressed in Chinese hamster ovary cells*. J Biol Chem, 1990. **265**(18): p. 10373-82.
55. Auwerx, J., et al., *Glycan deletions in the HIV-1 gp120 V1/V2 domain compromise viral infectivity, sensitize the mutant virus strains to carbohydrate-binding agents and represent a specific target for therapeutic intervention*. Virology, 2008. **382**(1): p. 10-9.
56. Liu, Y., et al., *Env length and N-linked glycosylation following transmission of human immunodeficiency virus Type 1 subtype B viruses*. Virology, 2008. **374**(2): p. 229-33.
57. Zhang, H., et al., *Restricted genetic diversity of HIV-1 subtype C envelope glycoprotein from perinatally infected Zambian infants*. PLoS One, 2010. **5**(2): p. e9294.
58. *Life expectancy of individuals on combination antiretroviral therapy in high-income countries: a collaborative analysis of 14 cohort studies*. Lancet, 2008. **372**(9635): p. 293-9.
59. Alexaki, A., Y. Liu, and B. Wigdahl, *Cellular reservoirs of HIV-1 and their role in viral persistence*. Curr HIV Res, 2008. **6**(5): p. 388-400.
60. Belmonte, L., et al., *Reservoirs of HIV replication after successful combined antiretroviral treatment*. Curr Med Chem, 2003. **10**(4): p. 303-12.
61. McNamara, L.A. and K.L. Collins, *Hematopoietic stem/precursor cells as HIV reservoirs*. Curr Opin HIV AIDS, 2011. **6**(1): p. 43-8.
62. Shen, L. and R.F. Siliciano, *Viral reservoirs, residual viremia, and the potential of highly active antiretroviral therapy to eradicate HIV infection*. J Allergy Clin Immunol, 2008. **122**(1): p. 22-8.
63. Mavigner, M., et al., *HIV-1 residual viremia correlates with persistent T-cell activation in poor immunological responders to combination antiretroviral therapy*. PLoS One, 2009. **4**(10): p. e7658.

64. Watson, C., et al., *The CCR5 receptor-based mechanism of action of 873140, a potent allosteric noncompetitive HIV entry inhibitor*. Mol Pharmacol, 2005. **67**(4): p. 1268-82.
65. Kitchen, C.M., et al., *Enfuvirtide antiretroviral therapy in HIV-1 infection*. Ther Clin Risk Manag, 2008. **4**(2): p. 433-9.
66. Fletcher, C.V., *Enfuvirtide, a new drug for HIV infection*. Lancet, 2003. **361**(9369): p. 1577-8.
67. Jamjian, M.C. and I.R. McNicholl, *Enfuvirtide: first fusion inhibitor for treatment of HIV infection*. Am J Health Syst Pharm, 2004. **61**(12): p. 1242-7.
68. Robertson, D., *US FDA approves new class of HIV therapeutics*. Nat Biotechnol, 2003. **21**(5): p. 470-1.
69. Dorr, P., et al., *Maraviroc (UK-427,857), a potent, orally bioavailable, and selective small-molecule inhibitor of chemokine receptor CCR5 with broad-spectrum anti-human immunodeficiency virus type 1 activity*. Antimicrob Agents Chemother, 2005. **49**(11): p. 4721-32.
70. Symons, J., et al., *Maraviroc is able to inhibit dual-R5 viruses in a dual/mixed HIV-1-infected patient*. J Antimicrob Chemother, 2011. **66**(4): p. 890-5.
71. Soriano, V., et al., *Optimal use of maraviroc in clinical practice*. AIDS, 2008. **22**(17): p. 2231-40.
72. Castonguay, L.A., et al., *Binding of 2-aryl-4-(piperidin-1-yl)butanamines and 1,3,4-trisubstituted pyrrolidines to human CCR5: a molecular modeling-guided mutagenesis study of the binding pocket*. Biochemistry, 2003. **42**(6): p. 1544-50.
73. Kuritzkes, D.R., *HIV-1 entry inhibitors: an overview*. Curr Opin HIV AIDS, 2009. **4**(2): p. 82-7.
74. Dimitrov, A., *Ibalizumab, a CD4-specific mAb to inhibit HIV-1 infection*. Curr Opin Investig Drugs, 2007. **8**(8): p. 653-61.
75. Bruno, C.J. and J.M. Jacobson, *Ibalizumab: an anti-CD4 monoclonal antibody for the treatment of HIV-1 infection*. J Antimicrob Chemother, 2010. **65**(9): p. 1839-41.
76. Song, R., et al., *Epitope mapping of ibalizumab, a humanized anti-CD4 monoclonal antibody with anti-HIV-1 activity in infected patients*. J Virol, 2010. **84**(14): p. 6935-42.
77. Jacobson, J.M., et al., *Safety, pharmacokinetics, and antiretroviral activity of multiple doses of ibalizumab (formerly TNX-355), an anti-CD4 monoclonal antibody, in human immunodeficiency virus type 1-infected adults*. Antimicrob Agents Chemother, 2009. **53**(2): p. 450-7.
78. Kuritzkes, D.R., et al., *Antiretroviral activity of the anti-CD4 monoclonal antibody TNX-355 in patients infected with HIV type 1*. J Infect Dis, 2004. **189**(2): p. 286-91.
79. Chiba, H., et al., *Actinohivin, a novel anti-human immunodeficiency virus protein from an actinomycete, inhibits viral entry to cells by binding high-mannose type sugar chains of gp120*. Biochem Biophys Res Commun, 2004. **316**(1): p. 203-10.

80. Bewley, C.A. and S. Otero-Quintero, *The potent anti-HIV protein cyanovirin-N contains two novel carbohydrate binding sites that selectively bind to Man(8) D1D3 and Man(9) with nanomolar affinity: implications for binding to the HIV envelope protein gp120*. J Am Chem Soc, 2001. **123**(17): p. 3892-902.
81. Moulaei, T., et al., *Monomerization of viral entry inhibitor griffithsin elucidates the relationship between multivalent binding to carbohydrates and anti-HIV activity*. Structure, 2010. **18**(9): p. 1104-15.
82. Abbas, A., et al., Cellular and Molecular immunology, Philadelphia, PA: Elsevier Press, 2010.
83. Abud-Mendoza, C. and R. Gonzalez-Amaro, *Rituximab in systemic lupus erythematosus*. Lupus, 2010. **19**(5): p. 658.
84. Kopp, M.V., *Omalizumab: Anti-IgE Therapy in Allergy*. Curr Allergy Asthma Rep, 2011. **11**(2): p. 101-6.
85. Cox, L., et al., *American Academy of Allergy, Asthma & Immunology/American College of Allergy, Asthma and Immunology Joint Task Force Report on omalizumab-associated anaphylaxis*. J Allergy Clin Immunol, 2007. **120**(6): p. 1373-7.
86. *Rituximab (Rituxan) for rheumatoid arthritis*. Med Lett Drugs Ther, 2006. **48**(1233): p. 34-5.
87. Garman, R.D., K. Munroe, and S.M. Richards, *Methotrexate reduces antibody responses to recombinant human alpha-galactosidase A therapy in a mouse model of Fabry disease*. Clin Exp Immunol, 2004. **137**(3): p. 496-502.
88. Ziolkowska, N.E., et al., *Crystallographic, thermodynamic, and molecular modeling studies of the mode of binding of oligosaccharides to the potent antiviral protein griffithsin*. Proteins, 2007. **67**(3): p. 661-70.
89. Ziolkowska, N.E., et al., *Domain-swapped structure of the potent antiviral protein griffithsin and its mode of carbohydrate binding*. Structure, 2006. **14**(7): p. 1127-35.
90. Ziolkowska, N.E., et al., *Crystallographic studies of the complexes of antiviral protein griffithsin with glucose and N-acetylglucosamine*. Protein Sci, 2007. **16**(7): p. 1485-9.
91. Giomarelli, B., et al., *Recombinant production of anti-HIV protein, griffithsin, by auto-induction in a fermentor culture*. Protein Expr Purif, 2006. **47**(1): p. 194-202.
92. O'Keefe, B.R., et al., *Scaleable manufacture of HIV-1 entry inhibitor griffithsin and validation of its safety and efficacy as a topical microbicide component*. Proc Natl Acad Sci U S A, 2009. **106**(15): p. 6099-104.
93. Montefiori, D.C., *Evaluating neutralizing antibodies against HIV, SIV, and SHIV in luciferase reporter gene assays*. Curr Protoc Immunol, 2005. **Chapter 12**: p. Unit 12 11.
94. Anderson, N.L., et al., *The human plasma proteome: a nonredundant list developed by combination of four separate sources*. Mol Cell Proteomics, 2004. **3**(4): p. 311-26.

95. Anderson, N.L. and N.G. Anderson, *The human plasma proteome: history, character, and diagnostic prospects*. Mol Cell Proteomics, 2002. **1**(11): p. 845-67.
96. Garbett, N.C., et al., *Differential scanning calorimetry of blood plasma for clinical diagnosis and monitoring*. Exp Mol Pathol, 2009. **86**(3): p. 186-91.
97. Garbett, N.C., et al., *Interrogation of the plasma proteome with differential scanning calorimetry*. Clin Chem, 2007. **53**(11): p. 2012-4.
98. Fish, D.J., et al., *Statistical analysis of plasma thermograms measured by differential scanning calorimetry*. Biophys Chem, 2010. **152**(1-3): p. 184-90.
99. Chaires, J.B., *Calorimetry and thermodynamics in drug design*. Annu Rev Biophys, 2008. **37**: p. 135-51.
100. Garbett, N.C., et al., *Calorimetry outside the box: a new window into the plasma proteome*. Biophys J, 2008. **94**(4): p. 1377-83.
101. Zhou, M., et al., *An investigation into the human serum "interactome"*. Electrophoresis, 2004. **25**(9): p. 1289-98.
102. Garbett, N.C., et al., *Calorimetric analysis of the plasma proteome*. Semin Nephrol, 2007. **27**(6): p. 621-6.
103. Fung, K.Y., et al., *A comprehensive characterization of the peptide and protein constituents of human seminal fluid*. Prostate, 2004. **61**(2): p. 171-81.
104. Shaw, J.L., C.R. Smith, and E.P. Diamandis, *Proteomic analysis of human cervico-vaginal fluid*. J Proteome Res, 2007. **6**(7): p. 2859-65.
105. Owen, D.H. and D.F. Katz, *A vaginal fluid simulant*. Contraception, 1999. **59**(2): p. 91-5.
106. Owen, D.H. and D.F. Katz, *A review of the physical and chemical properties of human semen and the formulation of a semen simulant*. J Androl, 2005. **26**(4): p. 459-69.
107. Fikkert, V., et al., *env chimeric virus technology for evaluating human immunodeficiency virus susceptibility to entry inhibitors*. Antimicrob Agents Chemother, 2002. **46**(12): p. 3954-62.
108. Wei, X., et al., *Antibody neutralization and escape by HIV-1*. Nature, 2003. **422**(6929): p. 307-12.
109. Platt, E.J., et al., *Effects of CCR5 and CD4 cell surface concentrations on infections by macrophagetropic isolates of human immunodeficiency virus type 1*. J Virol, 1998. **72**(4): p. 2855-64.
110. Wei, X., et al., *Emergence of resistant human immunodeficiency virus type 1 in patients receiving fusion inhibitor (T-20) monotherapy*. Antimicrob Agents Chemother, 2002. **46**(6): p. 1896-905.
111. Balzarini, J., et al., *Profile of resistance of human immunodeficiency virus to mannose-specific plant lectins*. J Virol, 2004. **78**(19): p. 10617-27.

APPENDIX

List of Abbreviations

GRFT	Griffithsin
HIV	Human Immunodeficiency Virus
HCV	Hepatitis C Virus
SARS	Severe Acute Respiratory Syndrome
Asn	Asparagine
Ser	Serine
Thr	Threonine
ER	Endoplasmic Reticulum
DNA	Deoxyribonucleic Acid
HAART	Highly Active Anti Retroviral Therapy
PBS	Phosphate Buffered Saline
CBC	Complete Blood Count
BSA	Bovine Serum Albumin
SDS	Sodium Dodecyl Sulfate
PAGE	Polyacrylamide Gel Electrophoresis
PVDF	Polyvinylidene Fluoride

CAPS	<i>N</i> -cyclohexyl-3-aminopropanesulfonic acid
NFDM	Nonfat Dry Milk
WBC	White Blood Cell
Ne	Neutrophils
Ly	Lymphocytes
Mo	Monocytes
Eo	Eosinophils
Ba	Basophils
RBC	Red Blood Cells
Hb	Hemoglobin
HCT	Hematocrit
MCV	Mean Corpuscular Volume
MCH	Mean Corpuscular Hemoglobin
MCHC	Mean Corpuscular Hemoglobin Concentration
RDW	Red Cell Distribution Width
MPV	Mean Platelet Volume
ALB	Albumin
ALKP	Alkaline Phosphatase
AMY	Amylase
DAPI	4',6-diamidino-2-phenylindole
PHA	Phytohemagglutinin
ANOVA	Analysis of Variance
DSC	Differential Scanning Calorimetry

CO-IP	Co-Immunoprecipitation
BCA	Bicinchoninic Acid
BGG	Bovine Gamma Globulin
NLGS	N-Linked Glycosylation Site

CURRICULUM VITA

BIOGRAPHICAL

Name: Christopher Lynn Barton **Birth Date:** 07-29-1976
Home Address: 206 Oxford Place **Birth Place:** Elgin, IL
Louisville, KY 40202
Home Phone: 502-418-2016
Business Address: Dept. of Pharmacology **Citizenship:** USA
E-Mail: Clbart01@louisville.edu
Business Phone: 502-852-2303

EDUCATION AND TRAINING

UNDERGRADUATE

<i>Dates attended Major Subject</i>	<i>Name and location of institution</i>	<i>Degree received and date</i>
1994-1998 Biology	University of Louisville Louisville, KY	Bachelor of Arts May 1998

GRADUATE

<i>Dates attended Major Subject</i>	<i>Name and location of institution</i>	<i>Degree received and date</i>
1999-2002 Law	University of Louisville Louisville, KY	Juris Doctor May 2002

2009-Present Pharmacology & Toxicology	University of Louisville Louisville, KY	Masters of Science August 2011
--	--	-----------------------------------

PROFESSIONAL EXPERIENCE

Years	Name and Location	Title
2008-2009	Barton Law Office, PLLC Louisville, KY	Attorney
2005-2008	Kentucky Office of Insurance Frankfort, KY	Attorney/Division Director
2004-2005	Barton Law Office, PLLC Louisville, KY	Attorney
2003-2004	CNAC Louisville, KY	In-House Counsel

MEMBERSHIPS in PROFESSIONAL and SCIENTIFIC SOCIETIES

Organization	Year
Kentucky Bar Association	2002-present
United States Patent and Trademark Office	2002-present
